Shape optimization for interface identification in nonlocal models

Matthias Schuster[1] · **Christian Vollmann**[1] · **Volker Schulz**[1]

Abstract

Shape optimization methods have been proven useful for identifying interfaces in models governed by partial differential equations. Here we consider a class of shape optimization problems constrained by nonlocal equations which involve interface–dependent kernels. We derive a novel shape derivative associated to the nonlocal system model and solve the problem by established numerical techniques. The code for obtaining the results in this paper is published at (https://github.com/schustermatthias/nlshape).

1 Introduction

Many physical relations and data-based coherences cannot satisfactorily be described by classical differential equations. Often they inherently possess some features, which are not purely local. In this regard, mathematical models which are governed by nonlocal operators enrich our modeling spectrum and present useful alternatives as well as supplemental approaches. That is why they appear in a large variety of applications including among others, anomalous or fractional diffusion [10, 11, 19], peridynamics [25, 27, 54, 64], image processing [31, 38, 42], cardiology [14], machine learning [44], as well as finance and jump processes [5, 6, 26, 37, 59]. Nonlocal operators are integral operators allowing for interactions between two distinct points in space. The nonlocal models investigated in this paper involve kernels that are not necessarily

✉ Volker Schulz
  volker.schulz@uni-trier.de

  Matthias Schuster
  schusterm@uni-trier.de

  Christian Vollmann
  vollmann@uni-trier.de

1 Universitaet Trier, 54286 Trier, Germany

Ⓐ Springer

symmetric and which are assumed to have a finite range of nonlocal interactions; see, e.g, [23, 24, 26, 60] and the references therein.

Not only the problem itself but also various optimization problems involving non-local models of this type are treated in literature. For example matching-type problems are treated in [18, 20, 21] to identify system parameters such as the forcing term or a scalar diffusion parameter. The control variable is typically modeled to be an element of a suitable function space. Moreover, nonlocal interface problems have become popular in recent years [13, 17, 29, 32, 43]. However, shape optimization techniques applied to nonlocal models can hardly be found in literature. For instance, the articles [9, 41, 55] deal with minimizing (functions of) eigenvalues of the fractional Laplacian with respect to the domain of interest. Also, in [8, 15] the energy functional related to fractional equations is minimized. In [12] a functional involving a more general kernel is considered. All of the aforementioned papers are of theoretical nature only. To the best of our knowledge, shape optimization problems involving nonlocal constraint equations with truncated kernels and numerical methods for solving such problems cannot yet be found in literature.

Instead, shape optimization problems which are constrained by partial differential equations appear in many fields of application [34, 46, 52, 53] and particularly for inverse problems where the parameter to be estimated, e.g., the diffusivity in a heat equation model, is assumed to be defined piecewise on certain subdomains. Given a rough picture of the configuration, shape optimization techniques can be successfully applied to identify the detailed shape of these subdomains [48–50, 62].

In this paper we transfer the problem of parameter identification into a nonlocal regime. Here, the parameter of interest is given by the kernel which describes the nonlocal model. We assume that this kernel is defined piecewise with respect to a given partition $\{\Omega_i\}_i$ of the domain of interest Ω. Thereby, the state of such a nonlocal model depends on the interfaces between the respective subdomains Ω_i. Under the assumption that we know the rough setting but are lacking in details, we can apply the techniques developed in the aforementioned shape optimization papers to identify these interfaces from a given measured state.

For this purpose we formulate a shape optimization problem which is constrained by an interface–dependent nonlocal convection–diffusion model. Here, we do not aim at investigating conceptual improvements of existing shape optimization algorithms. On the contrary, we want to study the applicability of established methods for problems of this type.

The realization of this plan basically requires two ingredients both of which are worked out here. First, we define a reasonable interface–dependent nonlocal model and provide a finite element code which discretizes a variational formulation thereof. Second, we need to derive the shape derivative of the corresponding nonlocal bilinear form which is then implemented into an overall shape optimization algorithm.

This leads to the following organization of the present paper. In Sect. 2 we formulate the shape optimization problem including an interface–dependent nonlocal model. Once established, we briefly recall basic concepts from the shape optimization regime in Sect. 3. Then Sect. 4 is devoted to the task of computing the shape derivative of the nonlocal bilinear form and the reduced objective functional. Finally we present numerical illustrations in Sect. 5 which corroborate theoretical findings.

2 Problem formulation

The system model to be considered is the *homogeneous steady-state nonlocal Dirichlet problem with volume constraints*, given by

$$\begin{cases} -\mathcal{L}_\Gamma u = f_\Gamma & \text{on } \Omega \\ \qquad u = 0 & \text{on } \Omega_I, \end{cases} \tag{1}$$

posed on a bounded domain $\Omega \subset \mathbb{R}^d$, $d \in \mathbb{N}$ and its nonlocal interaction domain Ω_I; see, e.g, [4, 23, 24, 26, 60] and the references therein. Here, we assume that this domain is partitioned into a simply connected interior subdomain $\Omega_1 \subset \Omega$ with boundary $\Gamma := \partial\Omega_1$ and a domain $\Omega_2 := \Omega\backslash\overline{\Omega}_1$. Thus we have $\Omega = \Omega(\Gamma) = \Omega_1\dot\cup\Gamma\dot\cup\Omega_2$, where $\dot\cup$ denotes the disjoint union. In the following, the boundary Γ of the interior domain Ω_1 is called the *interface* and is assumed to be an element of an appropriate shape space; see also Sect. 3 for a related discussion. The governing operator $\mathcal{L}_\Gamma$ is an *interface–dependent, nonlocal convection–diffusion operator* of the form

$$-\mathcal{L}_\Gamma u(\mathbf{x}) := \int_{\mathbb{R}^d} (u(\mathbf{x})\gamma_\Gamma(\mathbf{x}, \mathbf{y}) - u(\mathbf{y})\gamma_\Gamma(\mathbf{y}, \mathbf{x})) \, d\mathbf{y}, \tag{2}$$

which is determined by a nonnegative, interface–dependent *(interaction) kernel* $\gamma_\Gamma \colon \mathbb{R}^d \times \mathbb{R}^d \to \mathbb{R}$. The second equation in (1) is called *Dirichlet volume constraint*. It specifies the values of u on the *interaction domain*

$$\Omega_I := \left\{ \mathbf{y} \in \mathbb{R}^d\backslash\Omega \colon \exists\mathbf{x} \in \Omega : \gamma_\Gamma(\mathbf{x}, \mathbf{y}) \neq 0 \right\},$$

which consists of all points in the complement of Ω that interact with points in Ω. For ease of exposition, we set $u = 0$ on Ω_I, but generally we can use the constraint $u = g$ on Ω_I, if g satisfies some appropriate regularity assumptions.

Furthermore, we assume that the kernel depends on the interface in the following way

$$\gamma_\Gamma(\mathbf{x}, \mathbf{y}) = \sum_{i,j=1,2} \gamma_{ij}(\mathbf{x}, \mathbf{y})\chi_{\Omega_i \times \Omega_j}(\mathbf{x}, \mathbf{y}) + \sum_{i=1,2} \gamma_{iI}(\mathbf{x}, \mathbf{y})\chi_{\Omega_i \times \Omega_I}(\mathbf{x}, \mathbf{y}), \tag{3}$$

where $\chi_{\Omega_i \times \Omega_j}$ denotes the indicator of the set $\Omega_i \times \Omega_j$. For instance, in [51] the authors refer to γ_{ij} and γ_{iI} as inter– and intra–material coefficients. Notice that we do not need kernels γ_{Ii}, since $u = 0$ on Ω_I. Furthermore, for $i = 1, 2$ let $\{S_i(\mathbf{x})\}_{\mathbf{x}\in\Omega}$, with $S_i(\mathbf{x}) \subset \mathbb{R}^d$ for $\mathbf{x} \in \Omega$, be a family of sets, where the symmetry $\mathbf{y} \in S_i(\mathbf{x}) \Leftrightarrow \mathbf{x} \in S_i(\mathbf{y})$ for $\mathbf{x}, \mathbf{y} \in \Omega$ holds. We additionally assume for $i \in \{1, 2\}$ that there exist two radii $0 < \varepsilon_i^1 \leq \varepsilon_i^2 < \infty$ such that $B_{\varepsilon_i^1}(\mathbf{x}) \subset S_i(\mathbf{x}) \subset B_{\varepsilon_i^2}(\mathbf{x})$ for all $\mathbf{x} \in \Omega$, where $B_{\varepsilon_i^k}(\mathbf{x})$ denotes the Euclidean ball of radius ε_i^k.

Throughout this work we consider truncated interaction kernels, which can be written as

$$\gamma_{ij}(\mathbf{x}, \mathbf{y}) = \phi_{ij}(\mathbf{x}, \mathbf{y})\chi_{S_i(\mathbf{x})}(\mathbf{y}) \text{ and } \gamma_{iI}(\mathbf{x}, \mathbf{y}) = \phi_{iI}(\mathbf{x}, \mathbf{y})\chi_{S_i(\mathbf{x})}(\mathbf{y}) \text{ for } i, j = 1, 2 \tag{4}$$

for appropriate positive functions $\phi_{ij}\colon \mathbb{R}^d \times \mathbb{R}^d \to \mathbb{R}$ and $\phi_{iI}\colon \mathbb{R}^d \times \mathbb{R}^d \to \mathbb{R}$, which we refer to as *kernel functions*. In this paper we differentiate between *square integrable kernels* and *singular symmetric kernels*. For square integrable kernels we require $\gamma_{ij} \in L^2(\Omega \times \Omega)$ and $\gamma_{iI} \in L^2(\Omega \times \Omega_I)$, which also implies $\gamma_\Gamma \in L^2((\Omega \cup \Omega_I) \times (\Omega \cup \Omega_I))$. We do not assume that (3) is symmetric for this type of kernels.

In the case of singular symmetric kernels we require the existence of constants $0 < \gamma_* \le \gamma^* < \infty$ and a fraction $s \in (0, 1)$, such that

$$\gamma_* \le \gamma(\mathbf{x}, \mathbf{y})||\mathbf{x} - \mathbf{y}||_2^{d+2s} \le \gamma^*$$

for $\mathbf{x} \in \Omega$ and $\mathbf{y} \in S_1(\mathbf{x}) \cup S_2(\mathbf{x})$. Also, since the singular kernel is required to be symmetric, the condition $\gamma(\mathbf{x}, \mathbf{y}) = \gamma(\mathbf{y}, \mathbf{x})$, and, respectively, $\phi_{12}(\mathbf{x}, \mathbf{y}) = \phi_{21}(\mathbf{y}, \mathbf{x})$, $\phi_{ii}(\mathbf{x}, \mathbf{y}) = \phi_{ii}(\mathbf{y}, \mathbf{x})$ has to hold. Because we do not need to define γ_{Ii}, as described above, there is no further symmetry condition for γ_{iI} required.

Example 2.1 One example of such a singular symmetric kernel is given by

$$\gamma_{ij}(\mathbf{x}, \mathbf{y}) := \frac{\sigma_{ij}(\mathbf{x}, \mathbf{y})}{||\mathbf{x} - \mathbf{y}||_2^{d+2s}} \chi_{B_\varepsilon(\mathbf{x})}(\mathbf{y}), \quad \gamma_{iI}(\mathbf{x}, \mathbf{y}) := \frac{\sigma_{iI}(\mathbf{x}, \mathbf{y})}{||\mathbf{x} - \mathbf{y}||_2^{d+2s}} \chi_{B_\varepsilon(\mathbf{x})}(\mathbf{y}),$$

for $i, j = 1, 2$,

where $s \in (0, 1), 0 < \varepsilon < \infty$ and the functions $\sigma_{ij}, \sigma_{iI}\colon \mathbb{R}^d \times \mathbb{R}^d \to \mathbb{R}$ are bounded from below and above by some positive constants, say γ_* and γ^*. Additionally, the σ_{ii} are assumed to be symmetric on $\Omega \times \Omega$ and $\sigma_{12}(\mathbf{x}, \mathbf{y}) = \sigma_{21}(\mathbf{y}, \mathbf{x})$ holds for $\mathbf{x}, \mathbf{y} \in \Omega \cup \Omega_I$.

For the forcing term f_Γ in (1) we assume a dependency on the interface in the following way

$$f_\Gamma(\mathbf{x}) := \begin{cases} f_1(\mathbf{x}) : & \mathbf{x} \in \Omega_1 \\ f_2(\mathbf{x}) : & \mathbf{x} \in \Omega_2, \end{cases} \tag{5}$$
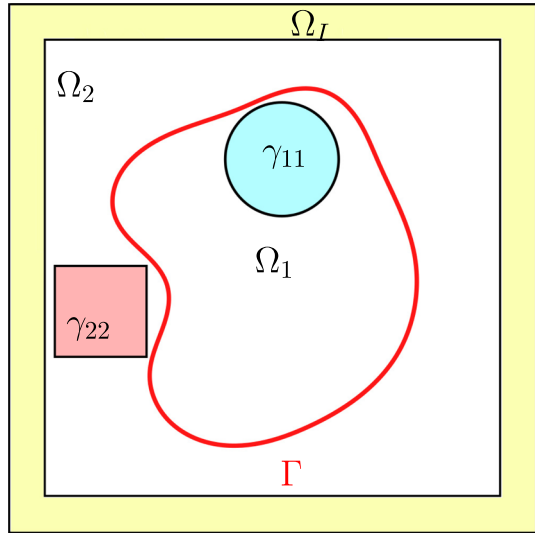
where we assume that $f_i \in H^1(\Omega)$, $i = 1, 2$, because we need that f is weakly differentiable in Sect. 4. Figure 1 illustrates our setting.

Next, we introduce a variational formulation of problem (1). For this purpose we define the corresponding forms

$$A_\Gamma(u, v) := (-\mathcal{L}_\Gamma u, v)_{L^2(\Omega)} \quad \text{and} \quad F_\Gamma(v) := (f_\Gamma, v)_{L^2(\Omega)} \tag{6}$$

for some functions $u, v\colon \Omega \cup \Omega_I \to \mathbb{R}$, where $v = 0$ on Ω_I. By inserting the definitions of the nonlocal operator (2) with the kernel given in (4) and the definition of the forcing term (5), we obtain the *nonlocal bilinear form*

Fig. 1 Here you can see one
example configuration, where
the domain Ω is divided in Ω_1
and Ω_2 with $\Gamma = \partial\Omega_1$ and Ω_I is
the nonlocal interaction domain.
In this case the support of
$\gamma_{11}(\mathbf{x}, \cdot)$ for one $\mathbf{x} \in \Omega_1$ is
depicted in blue and the support
of $\gamma_{22}(\mathbf{y}, \cdot)$ for one $\mathbf{y} \in \Omega_2$ is
colored in red, where the latter
can be expressed by using the
$||\cdot||_\infty$-ball in $\mathbb{R}^2$

$$A_\Gamma(u, v) = \int_\Omega v(\mathbf{x}) \int_{\mathbb{R}^d} (u(\mathbf{x})\gamma_\Gamma(\mathbf{x}, \mathbf{y}) - u(\mathbf{y})\gamma_\Gamma(\mathbf{y}, \mathbf{x})) d\mathbf{y} d\mathbf{x}$$

$$= \sum_{i,j=1,2} \int_{\Omega_i} v(\mathbf{x}) \int_{\Omega_j} \big(u(\mathbf{x})\gamma_{ij}(\mathbf{x}, \mathbf{y}) - u(\mathbf{y})\gamma_{ji}(\mathbf{y}, \mathbf{x})\big) d\mathbf{y} d\mathbf{x}$$

$$+ \sum_{i=1,2} \int_{\Omega_i} v(\mathbf{x})u(\mathbf{x}) \int_{\Omega_I} \gamma_{iI}(\mathbf{x}, \mathbf{y}) d\mathbf{y} d\mathbf{x} \tag{7}$$

$$= \sum_{i,j=1,2} \frac{1}{2} \int_{\Omega_i} \int_{\Omega_j} (v(\mathbf{x}) - v(\mathbf{y})) \big(u(\mathbf{x})\gamma_{ij}(\mathbf{x}, \mathbf{y}) - u(\mathbf{y})\gamma_{ji}(\mathbf{y}, \mathbf{x})\big) d\mathbf{y} d\mathbf{x}$$

$$+ \sum_{i=1,2} \int_{\Omega_i} v(\mathbf{x})u(\mathbf{x}) \int_{\Omega_I} \gamma_{iI}(\mathbf{x}, \mathbf{y}) d\mathbf{y} d\mathbf{x} \tag{8}$$

and the linear functional

$$F_\Gamma(v) = \int_\Omega f_\Gamma v \, d\mathbf{x} = \int_{\Omega_1} f_1 v \, d\mathbf{x} + \int_{\Omega_2} f_2 v \, d\mathbf{x}. \tag{9}$$

In order to derive the second bilinear form (8) we used Fubini's theorem. We employ both representations (7) and (8) of the nonlocal bilinear form in the proofs of Sect. 4. For singular symmetric kernels we also use another equivalent representation of the nonlocal bilinear form given by

$$A_\Gamma(u, v) = \frac{1}{2} \iint_{(\Omega\cup\Omega_I)^2} (v(\mathbf{x}) - v(\mathbf{y}))(u(\mathbf{x}) - u(\mathbf{y}))\gamma_\Gamma(\mathbf{x}, \mathbf{y}) \, d\mathbf{y} d\mathbf{x},$$

where we again used Fubini's theorem and applied that $u, v = 0$ on Ω_I. Next, we employ the nonlocal bilinear form to define a seminorm

$$|||u||| := \sqrt{A_\Gamma(u, u)}.$$

With this seminorm, we further define the energy spaces

$$V(\Omega \cup \Omega_I) := \{u \in L^2(\Omega \cup \Omega_I) : ||u||_{V(\Omega \cup \Omega_I)} := |||u||| + ||u||_{L^2(\Omega \cup \Omega_I)} < \infty\} \text{ and}$$
$$V_c(\Omega \cup \Omega_I) := \{u \in V(\Omega \cup \Omega_I) : u = 0 \text{ on } \Omega_I\}. \tag{10}$$

We now formulate the variational formulation corresponding to problem (1) as follows

$$\begin{aligned} given \; f_\Gamma \in H^1(\Omega) \; find \; u &\in V_c(\Omega \cup \Omega_I) \; such \; that \\ A_\Gamma(u, v) = F_\Gamma(v) \; &for \; all \; v \in V_c(\Omega \cup \Omega_I). \end{aligned} \tag{11}$$

Additionally, for $s \in (0, 1)$ we define the seminorm

$$|u|_{H^s(\Omega \cup \Omega_I)} := \int_{\Omega \cup \Omega_I} \int_{\Omega \cup \Omega_I} \frac{(u(\mathbf{x}) - u(\mathbf{y}))^2}{||\mathbf{x} - \mathbf{y}||_2^{d+2s}} \, d\mathbf{y} d\mathbf{x}$$

and the fractional Sobolev space as

$$\begin{aligned} H^s(\Omega \cup \Omega_I) := \{u \in L^2(\Omega \cup \Omega_I) : ||u||_{H^s(\Omega \cup \Omega_I)} \\ := ||u||_{L^2(\Omega \cup \Omega_I)} + |u|_{H^s(\Omega \cup \Omega_I)} < \infty\}. \end{aligned}$$

Moreover, we denote the volume-constrained spaces by

$$\begin{aligned} L_c^2(\Omega \cup \Omega_I) &:= \{u \in L^2(\Omega \cup \Omega_I) : u = 0 \text{ on } \Omega_I\} \text{ and} \\ H_c^s(\Omega \cup \Omega_I) &:= \{u \in H^s(\Omega \cup \Omega_I) : u = 0 \text{ on } \Omega_I\} \text{ for } s \in (0, 1). \end{aligned}$$

Then, for square integrable kernels one can show the equivalence between $\left(V(\Omega \cup \Omega_I), || \cdot ||_{V(\Omega \cup \Omega_I)}\right)$ and $\left(L^2(\Omega \cup \Omega_I), || \cdot ||_{L^2(\Omega \cup \Omega_I)}\right)$, i.e., there exist constants $C_1, C_2 > 0$ such that

$$C_1 ||u||_{L^2(\Omega \cup \Omega_I)} \leq ||u||_{V(\Omega \cup \Omega_I)} \leq C_2 ||u||_{L^2(\Omega \cup \Omega_I)}$$

and consequently $u \in V(\Omega \cup \Omega_I) \Leftrightarrow u \in L^2(\Omega \cup \Omega_I)$. Additionally, one can proof the equivalence of $(V_c(\Omega \cup \Omega_I), ||| \cdot |||)$ and $\left(L_c^2(\Omega \cup \Omega_I), || \cdot ||_{L^2(\Omega \cup \Omega_I)}\right)$, see related results in [24, 28, 61]. Moreover, the well-posedness of problem (11) for symmetric (square integrable) kernels is proven in [24] and in [28] the well-posedness for some nonsymmetric cases is also covered (again under certain conditions on the kernel and the forcing term f). For the singular symmetric kernels the well-posedness of problem (11), the equivalence between $\left(V(\Omega \cup \Omega_I), || \cdot ||_{V(\Omega \cup \Omega_I)}\right)$ and the fractional

Sobolev space $\left(H^s(\Omega \cup \Omega_I), ||\cdot||_{H^s(\Omega \cup \Omega_I)}\right)$ and between $(V_c(\Omega \cup \Omega_I), |||\cdot|||)$ and $\left(H_c^s(\Omega \cup \Omega_I), |\cdot|_{H^s(\Omega \cup \Omega_I)}\right)$ is shown in [24].

Finally, let us suppose we are given measurements $\bar{u} \colon \Omega \to \mathbb{R}$ on the domain Ω, which we assume to follow the nonlocal model (11) with the interface–dependent kernel γ_Γ and the forcing term f_Γ defined in (3) and (5), respectively. In order to formulate the shape derivative in Chapter 4 we need $\bar{u} \in H^1(\Omega)$. Then, given the data $\bar{u}$ we aim at identifying the interface Γ for which the corresponding nonlocal solution $u(\Gamma)$ is the "best approximation" to these measurements. Mathematically spoken, we formulate an optimal control problem with a tracking-type objective functional where the interface Γ represents the control variable and is modeled as an element of a shape space $\mathcal{A}$, which will be specified in Chapter 3.1. We now assume $\Omega := (0, 1)^2$ and introduce the following nonlocally constrained shape optimization problem

$$
\begin{aligned}
&\min_{\Gamma \in \mathcal{A}} J(u, \Gamma) &&(12)\\
&\text{s.t. } u \in V_c(\Omega \cup \Omega_I):\\
&\quad A_\Gamma(u, v) = F_\Gamma(v) \quad \text{for all } v \in V_c(\Omega \cup \Omega_I).
\end{aligned}
$$

The objective functional is given by

$$
J(u, \Gamma) := j(u, \Gamma) + j_{reg}(\Gamma) := \frac{1}{2}\int_\Omega (u - \bar{u})^2 \, d\mathbf{x} + \nu \int_\Gamma 1 \, ds.
$$

The first term $j(u, \Gamma)$ is a standard L^2 tracking-type functional, whereas the second term $j_{reg}(\Gamma)$ is known as the perimeter regularization, which is commonly used in the related literature to overcome possible ill-posedness of optimization problems [3].

3 Basic concepts in shape optimization

For solving the constrained shape optimization problem (12) we want to use the same shape optimization algorithms as they are developed in [47, 48, 50] for problem classes that are comparable in structure. Thus, in this section we briefly introduce the basic concepts and ideas of the therein applied shape formalism. For a rigorous introduction to shape spaces, shape derivatives and shape calculus in general, we refer to the monographs [16, 56, 62]. From now on, we restrict ourselves to the cases $d \in \{2, 3\}$ for the remaining part of this paper, since shape optimization problems are typically formulated for a two- or three-dimensional setting.

3.1 Notations and definitions

Based on our perception of the interface, we now refer to the image of a simple closed and smooth sphere as a *shape*, i.e., the spaces of interest are subsets of

$$\mathcal{A} := \left\{ \Gamma := \varphi(S^{d-1}) \colon \varphi \in C^\infty(S^{d-1}, \Omega) \text{ injective; } \varphi' \neq 0 \right\}, \tag{13}$$

where S^{d-1} is the unit sphere in $\mathbb{R}^d$. By the Jordan-Brouwer separation theorem [33] such a shape $\Gamma \in \mathcal{A}$ divides the space into two (simply) connected components with common boundary Γ. One of them is the bounded interior, which in our situation can then be identified with Ω_1.

Functionals $J \colon \mathcal{A} \to \mathbb{R}$ which assign a real number to a shape are called *shape functionals*. Since this paper deals with minimizing such shape functionals, i.e., with so-called shape optimization problems, we need to introduce the notion of an appropriate *shape derivative*. To this end we consider a family of mappings $\mathbf{F_t} \colon \overline{\Omega} \to \mathbb{R}^d$ with $\mathbf{F_0} = \mathbf{id}$, where $t \in [0, T]$ and $T \in (0, \infty)$ sufficiently small, which transform a shape Γ into a family of *perturbed shapes* $\left\{\Gamma^t\right\}_{t \in [0,T]}$, where $\Gamma^t := \mathbf{F_t}(\Gamma)$ with $\Gamma^0 = \Gamma$. Here the family of mappings $\{\mathbf{F_t}\}_{t \in [0,T]}$ is described by the *perturbation of identity*, which for a smooth vector field $\mathbf{V} \in C_0^k(\Omega, \mathbb{R}^d)$, $k \in \mathbb{N}$, is defined by

$$\mathbf{F_t}(\mathbf{x}) := \mathbf{x} + t\mathbf{V}(\mathbf{x}), \quad \text{for all } \mathbf{x} \in \Omega.$$

We note that for sufficiently small $t \in [0, T]$ the function $\mathbf{F_t}$ is injective, and thus $\Gamma^t \in \mathcal{A}$. Then the *Eulerian or directional derivative* of a shape functional J at a shape Γ in direction of a vector field $\mathbf{V} \in C_0^k(\Omega, \mathbb{R}^d)$, $k \in \mathbb{N}$, is defined by

$$D_\Gamma J(\Gamma)[\mathbf{V}] := \left.\frac{d}{dt}\right|_{t=0^+} J(\mathbf{F_t}(\Gamma)) = \lim_{t \searrow 0} \frac{(J(\mathbf{F_t}(\Gamma)) - J(\Gamma))}{t}. \tag{14}$$

If $D_\Gamma J(\Gamma)[\mathbf{V}]$ exists for all $\mathbf{V} \in C_0^k(\Omega, \mathbb{R}^d)$, $\mathbf{V} \mapsto DJ(\Gamma)[\mathbf{V}]$ is continuous and in the dual space $\left(C_0^k(\Omega, \mathbb{R}^d)\right)^*$, then $DJ(\Gamma)[\mathbf{V}]$ is called the *shape derivative* of J [62, Definition 4.6].

At this point, let us also define the *material derivative* of a family of functions $\{v^t \colon \Omega \to \mathbb{R} : t \in [0, T]\}$ in direction $\mathbf{V}$ by

$$D_m v(\mathbf{x}) := \left.\frac{d}{dt}\right|_{t=0^+} v^t(\mathbf{F_t}(\mathbf{x})).$$

For functions v, which do not explicitly depend on the shape, i.e., $v^t = v$ for all $t \in [0, T]$, we find

$$D_m v = \nabla v^\top \mathbf{V}.$$

For more details on shape optimization we refer to the literature, e.g., [16] or [56].

Remark 3.1 In case of the nonlocal problem (12) we extend the vector field $\mathbf{V}$ to $\Omega \cup \Omega_I$ by zero, i.e, $\mathbf{V} \in C_0^k(\Omega \cup \Omega_I, \mathbb{R}^d) := \{\mathbf{V} : \Omega \cup \Omega_I \to \mathbb{R}^d : \mathbf{V}|_{\Omega} \in C_0^k(\Omega, \mathbb{R}^d)$ and $\mathbf{V} = 0$ on $\Omega_I\}$. Accordingly, the shape of the interaction domain Ω_I does not change. Moreover, in this work $\mathbf{V} \in C_0^1(\Omega \cup \Omega_I, \mathbb{R}^d)$ is sufficient for all computations.

3.2 Optimization approach: averaged adjoint method

Let us assume, that for each admissible shape Γ, there exists a unique solution $u(\Gamma)$ of the constraint equation, i.e., $u(\Gamma)$ satisfies $A_\Gamma(u(\Gamma), v) = F_\Gamma(v)$ for all $v \in V_c(\Omega \cup \Omega_I)$. Then we can consider the *reduced problem*

$$\min_\Gamma J^{red}(\Gamma) := J(u(\Gamma), \Gamma). \tag{15}$$

In order to employ derivative based minimization algorithms, we need to derive the shape derivative of the reduced objective functional J^{red}. By formally applying the chain rule, we obtain

$$D_\Gamma J^{red}(\Gamma)[\mathbf{V}] = D_u J(u(\Gamma), \Gamma) D_\Gamma u(\Gamma)[\mathbf{V}] + D_\Gamma J(u(\Gamma), \Gamma)[\mathbf{V}],$$

where $D_u J$ and $D_\Gamma J$ denote the partial derivatives of the objective J with respect to the state variable u and the control Γ, respectively. In applications we typically do not have an explicit formula for the control-to-state mapping $u(\Gamma)$, so that we cannot analytically quantify the sensitivity of the unique solution $u(\Gamma)$ with respect to the interface Γ. Thus, a formula for the shape derivative $D_\Gamma u(\Gamma)[\mathbf{V}]$ is unattainable. One possible approach to circumvent $D_\Gamma u(\Gamma)[\mathbf{V}]$ and access the shape derivative $D_\Gamma J^{red}(\Gamma)[\mathbf{V}]$ is the *averaged adjoint method (AAM)* developed in [36, 57, 58], which is a Lagrangian method, where the so-called *Lagrangian functional* is defined as

$$L(u, \Gamma, v) := J(u, \Gamma) + A_\Gamma(u, v) - F_\Gamma(v).$$

The basic idea behind Lagrangian methods is the aspect, that we can express the reduced functional as

$$J^{red}(\Gamma) = L(u(\Gamma), \Gamma, v), \quad \forall v \in V_c(\Omega \cup \Omega_I).$$

Now let Γ be fixed and denote by $\Gamma^t := \mathbf{F_t}(\Gamma)$ and $\Omega_i^t := \mathbf{F_t}(\Omega_i)$ the deformed interior boundary and the deformed domains, respectively. Furthermore we indicate by writing $\Omega(\Gamma^t)$ that we use the decomposition $\Omega(\Gamma^t) = \Omega_1^t \cup \Gamma^t \cup \Omega_2^t \, (= \Omega)$, where $\Gamma^t = \partial\Omega_1^t$. Consequently, the norm $||\cdot||_{V(\Omega(\Gamma^t)\cup\Omega_I)}$ of the space $V(\Omega(\Gamma^t) \cup \Omega_I)$ differs from the norm $||\cdot||_{V(\Omega\cup\Omega_I)}$ of the space $V(\Omega \cup \Omega_I)$ due to the interface-sensitivity of the kernel, see (10). Then we consider the reduced objective functional regarding Γ^t, i.e.,

$$J^{red}(\Gamma^t) = L(u(\Gamma^t), \Gamma^t, v), \quad \forall v \in V_c(\Omega(\Gamma^t) \cup \Omega_I), \tag{16}$$

where $u(\Gamma^t) \in V_c(\Omega(\Gamma^t) \cup \Omega_I)$. If we now try to differentiate L with respect to t in order to derive the shape derivative, we would have to compute the derivative for $u(\Gamma^t) \circ \mathbf{F_t}$ and $v \circ \mathbf{F_t}$, where $u(\Gamma^t), v \in V_c(\Omega(\Gamma^t) \cup \Omega_I)$ may not be differentiable. Additionally the norm $|| \cdot ||_{V(\Omega(\Gamma^t) \cup \Omega_I)}$, and therefore the space $V_c(\Omega(\Gamma^t) \cup \Omega_I)$, is also dependent on t. Instead, since $\mathbf{F_t}$ is a homeomorphism, we can use that for $u, v \in V_c(\Omega(\Gamma^t) \cup \Omega_I)$, there exist functions $\tilde{u}, \tilde{v} \in V_c(\Omega \cup \Omega_I)$, such that

$$u = \tilde{u} \circ \mathbf{F_t}^{-1} \text{ and } v = \tilde{v} \circ \mathbf{F_t}^{-1}.$$

Moreover let $T \in (0, \infty)$ be sufficiently small. Then we define

$$
\begin{aligned}
&J : [0, T] \times V_c(\Omega \cup \Omega_I) \to \mathbb{R}, \\
&\quad J(t, u) := J(u \circ \mathbf{F_t}^{-1}, \Gamma^t), \\
&\quad A : [0, T] \times V_c(\Omega \cup \Omega_I) \times V_c(\Omega \cup \Omega_I) \to \mathbb{R}, \\
&\quad A(t, u, v) := A_{\Gamma^t}(u \circ \mathbf{F_t}^{-1}, v \circ \mathbf{F_t}^{-1}), \\
&\quad F : [0, T] \times V_c(\Omega \cup \Omega_I) \to \mathbb{R}, \\
&\quad F(t, v) := F_{\Gamma^t}(v \circ \mathbf{F_t}^{-1}), \\
&\quad G : [0, T] \times V_c(\Omega \cup \Omega_I) \times V_c(\Omega \cup \Omega_I) \to \mathbb{R}, \\
&\quad G(t, u, v) := L(u \circ \mathbf{F_t}^{-1}, \Gamma^t, v \circ \mathbf{F_t}^{-1}) = J(t, u) + A(t, u, v) - F(t, v). \quad (17)
\end{aligned}
$$

Then we can reformulate (16) as

$$J^{red}(\Gamma^t) = G(t, u^t, v), \quad \forall v \in V_c(\Omega \cup \Omega_I),$$

where $u^t \in V_c(\Omega \cup \Omega_I)$ is the unique solution of the nonlocal equation corresponding to Γ^t

$$A(t, u, v) - F(t, v) = 0, \quad \forall v \in V_c(\Omega \cup \Omega_I).$$

Furthermore $A(t, u, v) - F(t, v)$ is obviously linear in v for all $(t, u) \in [0, T] \times V_c(\Omega \cup \Omega_I)$, which is one prerequisite of the AAM. Then, in order to use the AAM to compute the shape derivative, the following additional assumptions have to be met.

- **Assumption (H0)**: For every $(t, v) \in [0, T] \times V_c(\Omega \cup \Omega_I)$

  1. $[0, 1] \ni s \mapsto G(t, su^t + (1 - s)u^0, v)$ is absolutely continuous and
  2. $[0, 1] \ni s \mapsto d_u G(t, su^t + (1 - s)u^0, v)[\tilde{u}] \in L^1((0, 1))$ for all $\tilde{u} \in V_c(\Omega \cup \Omega_I)$.

- For every $t \in [0, T]$ there exists a unique solution $v^t \in L^2(\Omega)$, such that v^t solves the averaged adjoint equation

$$\int_0^1 d_u G(t, su^t + (1 - s)u^0, v^t)[\tilde{u}]ds = 0 \quad \text{for all } \tilde{u} \in V_c(\Omega \cup \Omega_I). \quad (18)$$

- **Assumption (H1)**:

  Assume that the following equation holds

$$\lim_{t \searrow 0} \frac{G(t, u^0, v^t) - G(0, u^0, v^t)}{t} = \partial_t G(0, u^0, v^0).$$

In our case, due to the linearity of $A(t, \tilde{u}, v^t)$ in the second argument, the left-hand side of the averaged adjoint equation (18) can be formulated as

$$\int_0^1 d_u G(t, su^t + (1 - s)u^0, v^t)[\tilde{u}] \, ds = A(t, \tilde{u}, v^t) + \int_\Omega \left(\frac{1}{2}(u^t + u^0) - \bar{u}^t \right) \tilde{u} \xi^t \, d\mathbf{x},$$

where $\xi^t(\mathbf{x}) := det \, D\mathbf{F_t}(\mathbf{x})$ and $\bar{u}^t(\mathbf{x}) := \bar{u}(\mathbf{F_t}(\mathbf{x}))$. As a consequence, (18) is equivalent to

$$\mathcal{A}(t, \tilde{u}, v^t) = -\int_\Omega \left(\frac{1}{2} \left(u^t + u^0 \right) - \bar{u}^t \right) \tilde{u} \xi^t \, d\mathbf{x} \quad \forall \tilde{u} \in V_c(\Omega \cup \Omega_I).$$

For $t = 0$ we get

$$A(0, \tilde{u}, v^0) = -\int_\Omega (u^0 - \bar{u})\tilde{u} \, d\mathbf{x} \quad \forall \tilde{u} \in V_c(\Omega \cup \Omega_I). \tag{19}$$

In this case we call (19) adjoint equation and the solution v^0 is referred to as the adjoint solution. Moreover the nonlocal problem (11) for $t = 0$ is also called state equation and the solution u^0 is named state solution.

Finally, the next theorem yields a practical formula for deriving the shape derivative.

Theorem 3.2 ([36, Theorem 3.1]) *Let the assumptions (H0) and (H1) be satisfied and suppose there exists a unique solution v^t to the averaged adjoint equation (18). Then for $v \in V_c(\Omega \cup \Omega_I)$ we obtain*

$$D_\Gamma J^{red}(\Gamma)[\mathbf{V}] = \left. \frac{d}{dt} \right|_{t=0^+} J^{red}(\Gamma^t) = \left. \frac{d}{dt} \right|_{t=0^+} G(t, u^t, v) = \partial_t G(0, u^0, v^0). \tag{20}$$

Proof See proof of [36, Theorem 3.1]. □

Remark 3.3 Under the assumption that the material derivatives of u and v exist and that $D_m u, D_m v \in V_c(\Omega \cup \Omega_I)$, one can also use the material derivative approach of [7] to derive the shape derivative of the reduced functional (15).

3.3 Optimization algorithm

Let us assume for a moment that we have an explicit formula for the shape derivative of the reduced objective functional. We now briefly recall the techniques developed

in [50] and describe how to exploit this derivative for implementing gradient based optimization methods or even Quasi-Newton methods, such as L-BFGS, to solve the constrained shape optimization problem (12).

In order to identify gradients we need to require the notion of an inner product, or more generally a Riemannian metric. Unfortunately, shape spaces typically do not admit the structure of a linear space. However, in particular situations it is possible to define appropriate quotient spaces, which can be equipped with a Riemannian structure. For instance consider the set $\mathcal{A}$ introduced in (13). Since we are only interested in the image of the defining embedding, a re-parametrization thereof does not lead to a different shape. Consequently, two spheres that are equal modulo (diffeomorphic) re-parametrizations define the same shape. This conception naturally leads to the quotient space $\mathrm{Emb}(S^{d-1}, \mathbb{R}^d) / \mathrm{Diff}(S^{d-1}, S^{d-1})$, which can be considered an infinite-dimensional Riemannian manifold [39, 62]. This example already intimates the difficulty of translating abstract shape derivatives into discrete optimization methods; see, e.g., the thesis [63] on this topic. A detailed discussion of these issues is not the intention of this work and we now outline Algorithm 1.

The basic idea can be intuitively explained in the following way. Starting with an initial guess Γ_0, we aim to iterate in a steepest-descent fashion over interfaces Γ_k until we reach a "stationary point" of the reduced objective functional J^{red}. The interface Γ_k is encoded in the finite element mesh and transformations thereof are realized by adding vector fields $\mathbf{U} \colon \Omega \to \mathbb{R}^d$ (which can be interpreted as tangent vectors at a fixed interface) to the finite element nodes which we denote by Ω_k.

Thus, the essential part is to update the finite element mesh after each iteration by adding an appropriate transformation vector field. For this purpose, we use the solution $\mathbf{U}(\Gamma) \colon \Omega(\Gamma) \to \mathbb{R}^d$ of the so-called *deformation equation*

$$a_\Gamma(\mathbf{U}(\Gamma), \mathbf{V}) = D_\Gamma J^{red}(\Gamma)[\mathbf{V}] \quad \text{for all } \mathbf{V} \in H_0^1(\Omega(\Gamma), \mathbb{R}^d). \tag{21}$$

The right-hand side of this equation is given by the shape derivative of the reduced objective functional (20) and the left-hand side denotes an inner product on the vector field space $H_0^1(\Omega, \mathbb{R}^d)$. In the view of the manifold interpretation, we can consider a_Γ as inner product on the tangent space at Γ, so that $\mathbf{U}(\Gamma)$ is interpretable as the gradient of the shape functional J^{red} at Γ. The solution $\mathbf{U}(\Gamma) \colon \Omega \to \mathbb{R}^d$ of (21) is then added in a scaled version to the coordinates Ω_k of the finite element nodes.
A common choice for a_Γ is the bilinear form associated to the linear elasticity equation given by

$$a_\Gamma(\mathbf{U}, \mathbf{V}) = \int_{\Omega(\Gamma)} \sigma(\mathbf{U}) : \epsilon(\mathbf{V}) \, dx,$$

for $\mathbf{U}, \mathbf{V} \in H_0^1(\Omega, \mathbb{R}^d)$ and the identity function $\mathbf{Id} : \mathbb{R}^d \to \mathbb{R}^d$, where

$$\sigma(\mathbf{U}) := \lambda \mathrm{tr}(\epsilon(\mathbf{U})) \, \mathbf{Id} + 2\mu\epsilon(\mathbf{U}) \tag{22}$$

and

$$\epsilon(\mathbf{U}) := \frac{1}{2}(\nabla\mathbf{U} + \nabla\mathbf{U}^T)$$

are the strain and stress tensors, respectively. Deformation vector fields $\mathbf{V}$ which do not change the interface do not have an impact on the reduced objective functional, so that

$$D_\Gamma J^{red}(\Gamma)[\mathbf{V}] = 0 \quad \text{for all } \mathbf{V} \text{ with } \operatorname{supp}(\mathbf{V}) \cap \Gamma = \emptyset.$$

Therefore, the right-hand side $D_\Gamma J^{red}(\Gamma)[\mathbf{V}]$ is only assembled for test vector fields whose support intersects with the interface Γ and set to zero for all other basis vector fields. This prevents wrong mesh deformations resulting from discretization errors as outlined and illustrated in [49]. Furthermore, λ and μ in (22) denote the Lamé parameters which do not need to have a physical meaning here. It is more important to understand their effect on the mesh deformation. They enable us to control the stiffness of the material and thus can be interpreted as some sort of step size. In [47], it is observed that locally varying Lamé parameters have a stabilizing effect on the mesh. A good strategy is to choose $\lambda = 0$ and μ as solution of the following Laplace equation

$$\begin{aligned}
-\Delta\mu &= 0 && \text{in } \Omega \\
\mu &= \mu_{\max} && \text{on } \Gamma \\
\mu &= \mu_{\min} && \text{on } \partial\Omega.
\end{aligned} \tag{23}$$

Therefore $\mu_{\min}, \mu_{\max} \in \mathbb{R}$ influence the step size of the optimization algorithm. A small step is achieved by the choice of a large $\mu_{\max}$. Note that a_Γ then depends on the interface Γ through the parameter $\mu = \mu(\Gamma): \Omega(\Gamma) \to \mathbb{R}$.

How to perform the limited memory L-BFGS update in Line 13 of Algorithm 1 within the shape formalism is investigated in [49, Section 4]. Here, we only mention that the therein examined vector transport is approximated with the identity operator, so that we finally treat the gradients $\mathbf{U}_k : \Omega_k \to \mathbb{R}^d$ as vectors in $\mathbb{R}^{d|\Omega_k|}$ and implement the standard L-BFGS update [47, Section 5]. For the sufficient decrease condition in Line 18 a small value for c, e.g., $c = 10^{-4}$, is suggested in [40].

4 Shape derivative of the reduced objective functional

In Sect. 3 we have depicted the optimization methodology, that we follow in this work to numerically solve the constrained shape optimization problem (12). First, we need the following conclusion from [56, Proposition 2.32].

Lemma 4.1 *If $\gamma \in W^{1,1}(\mathbb{R}^d \times \mathbb{R}^d, \mathbb{R})$ and $\tilde{\mathbf{V}} \in C_0^1(\mathbb{R}^d \times \mathbb{R}^d, \mathbb{R}^d \times \mathbb{R}^d)$, then $t \mapsto \gamma \circ \tilde{\mathbf{F}}_{\mathbf{t}}$, where $\tilde{\mathbf{F}}_{\mathbf{t}} := (\mathbf{x}, \mathbf{y}) + t\tilde{\mathbf{V}}(\mathbf{x}, \mathbf{y})$, is differentiable in $L^1(\mathbb{R}^d \times \mathbb{R}^d, \mathbb{R})$ and its derivative is given by*

Algorithm 1: Shape optimization algorithm

---

1 Initialize: γ_Γ, f_Γ, Γ^0, $\bar{u}$, $k = 1$, `maxiter` $\in \mathbb{N}$

2 **while** $k \leq$ `maxiter` *(alternatively* $\|DJ^{red}(\Gamma_k)\| > tol$*)* **do**

3   Interpolate $\bar{u}$ onto the current finite element mesh Ω_k

4   Assemble A_Γ and solve state (11) and adjoint equation (19)

5        $\rightarrow u(\Gamma_k), v(\Gamma_k)$

6   Compute the mesh deformation

7   Assemble shape derivative $D_\Gamma J^{red}(\Gamma_k)[\mathbf{V}] = D_\Gamma L(u(\Gamma_k), \Gamma_k, v(\Gamma_k))[\mathbf{V}]$ (20)

8   Set $D_\Gamma J^{red}(\Gamma_k)[\mathbf{V}] = 0$ for all $\mathbf{V}$ with supp$(\mathbf{V}) \cap \Gamma_k = \emptyset$

9   Compute locally varying Lamé parameter by solving (23)

10   Assemble linear elasticity a_{Γ_k} and solve the deformation equation (21)

11       $\rightarrow \mathbf{U}_k$

12   **if** *curvature condition is satisfied* **then**

13       $\tilde{\mathbf{U}}_k =$ L-BFGS-Update

14   **else**

15       $\tilde{\mathbf{U}}_k = -\mathbf{U}_k$

16   **end if**

17   Backtracking line search (with parameters $\alpha = 1$, $\tau, c \in (0, 1)$)

18   **while** $J^{red}((\mathbf{Id} + \alpha\tilde{\mathbf{U}}_k)(\Gamma_k)) > J^{red}(\Gamma_k) + cD_\Gamma J^{red}(\Gamma_k)[\tilde{\mathbf{U}}_k]$ **do**

19         $\alpha = \tau\alpha$

20   **end while**

21       $\rightarrow \alpha_k$

22   Update mesh

23       $\Omega_{k+1} = (\mathbf{Id} + \alpha_k\tilde{\mathbf{U}}_k)(\Omega_k)$

24     $k = k + 1$

25 **end while**

$$\left.\frac{d}{dt}\right|_{t=0} \gamma \circ \tilde{\mathbf{F}}_{\mathbf{t}} = \nabla\gamma^T\tilde{\mathbf{V}}.$$

Proof See proof of [56, Proposition 2.32]. □

Remark 4.2 Given a subset $D \subset \mathbb{R}^d \times \mathbb{R}^d$ of nonzero measure, we can replace the set $\mathbb{R}^d \times \mathbb{R}^d$ by D in Lemma 4.1 and the statement still holds, which can be proven by extending functions $\gamma \in W^{1,1}(D, \mathbb{R})$ and $\tilde{\mathbf{V}} \in C_0^1(D, D)$ by zero to functions $\hat{\gamma} \in W^{1,1}(\mathbb{R}^d \times \mathbb{R}^d, \mathbb{R})$ and $\hat{\mathbf{V}} \in C_0^1(\mathbb{R}^d \times \mathbb{R}^d, \mathbb{R}^d \times \mathbb{R}^d)$.

In our case, we set $\tilde{\mathbf{V}}(\mathbf{x}, \mathbf{y}) := (\mathbf{V}(\mathbf{x}), \mathbf{V}(\mathbf{y}))$ in order to use Lemma 4.1 to derive several derivatives in this section.

In order to prove the requirements of the AAM, we need some additional assumptions.

Assumption (P0):

- For every $t \in [0, T]$, there exist unique solutions $u^t, v^t \in V_c(\Omega \cup \Omega_I)$, such that

$$A(t, u^t, v) = F(t, v) \text{ for all } v \in V_c(\Omega \cup \Omega_I) \text{ and}$$

$$A(t, u, v^t) = \left(-(\frac{1}{2}(u^t + u^0) - \bar{u}^t)\xi^t, u\right)_{L^2(\Omega\cup\Omega_I)} \text{ for all } u \in V_c(\Omega \cup \Omega_I),$$

$$(24)$$

where $A(t, u, v)$ and $F(t, v)$ are defined as in (17), $\bar{u}^t(\mathbf{x}) := \bar{u}(\mathbf{F_t}(\mathbf{x}))$ and $\xi^t(\mathbf{x}) := \det D\mathbf{F_t}(\mathbf{x})$.

- Additionally assume that there exists a constant $0 < C_0 < \infty$, such that

$$A(t, u, u) \geq C_0 ||u||^2_{L^2(\Omega)} \text{ for all } t \in [0, T] \text{ and } u \in V_c(\Omega \cup \Omega_I),$$

where A is defined as in (17).

Assumption (P1):

For each class of kernels additional requirements have to hold:

- Define the sets $D_n := \{(\mathbf{x}, \mathbf{y}) \in (\Omega \cup \Omega_I)^2 : ||\mathbf{x} - \mathbf{y}||_2 > \frac{1}{n}\}$ for $n \in \mathbb{N}$.
  Then, singular kernels are assumed to have weak derivatives $\nabla_x \gamma, \nabla_y \gamma \in L^1(D_n, \mathbb{R}^d)$ for all $n \in \mathbb{N}$ with

$$|\nabla_\mathbf{x} \gamma_{ij}(\mathbf{x}, \mathbf{y})^\top \mathbf{V}(\mathbf{x}) + \nabla_\mathbf{y} \gamma_{ij}(\mathbf{x}, \mathbf{y})^\top \mathbf{V}(\mathbf{y})|||\mathbf{x} - \mathbf{y}||^{d+2s}_2 \in L^\infty(\Omega \times \Omega) \text{ and}$$
$$|\nabla_\mathbf{x} \gamma_{iI}(\mathbf{x}, \mathbf{y})^\top \mathbf{V}(\mathbf{x})|||\mathbf{x} - \mathbf{y}||^{d+2s}_2 \in L^\infty(\Omega \times \Omega_I).$$

- Square integrable kernels have to meet the following conditions

$$\gamma_{ij}, \nabla \gamma_{ij} \in L^\infty(\Omega \times \Omega) \text{ and}$$
$$\gamma_{iI}, \nabla \gamma_{iI} \in L^\infty(\Omega \times \Omega_I).$$

Remark 4.3 We recall that there exists a Lipschitz constant $L > 0$ such that

$$||\mathbf{F_t}^{-1}(\mathbf{x}) - \mathbf{F_t}^{-1}(\mathbf{y})||_2 \leq \frac{1}{L}||\mathbf{x} - \mathbf{y}||_2 \text{ for } \mathbf{x}, \mathbf{y} \in \Omega \cup \Omega_I \text{ and } t \in [0, T],$$

if $T > 0$ is chosen small enough. Consequently we derive

$$\gamma^t(\mathbf{x}, \mathbf{y}) = \gamma(\mathbf{F_t}(\mathbf{x}), \mathbf{F_t}(\mathbf{x})) \leq \frac{\gamma*}{||\mathbf{F_t}(\mathbf{x}) - \mathbf{F_t}(\mathbf{y})||^{d+2s}_2} \leq \frac{L\gamma*}{||\mathbf{x} - \mathbf{y}||^{d+2s}_2} \text{ for } \mathbf{x}, \mathbf{y} \in \Omega \cup \Omega_I.$$

Therefore $\gamma^t(\mathbf{x}, \mathbf{y}) \leq \frac{L\gamma*}{||\mathbf{x}-\mathbf{y}||^{d+2s}_2} < L\gamma^* n^{d+2s}$ for $(\mathbf{x}, \mathbf{y}) \in D_n$, $t \in [0, T]$ and we get $\gamma^t \in W^{1,1}(D_n, \mathbb{R})$ for singular symmetric kernels if Assumption (P1) is fulfilled.

Singular kernels already satisfy Assumption (P0) since the nonlocal equations in the first condition are well-posed, which can trivially be proven by using the theory of [24, 61]. Additionally, singular kernels also fulfill the second requirement of (P0), which is shown in the following Lemma:

Lemma 4.4 *In the case of a singular kernel, there exists a constant $0 < C_0 < \infty$, so that*

$$A(t, u, u) \geq C_0 ||u||_{L^2(\Omega)}, \quad \text{for every } t \in [0, T], \ u \in H^s(\Omega).$$

Proof Let $\varepsilon := \min\{\varepsilon_1^1, \varepsilon_2^1\}$. Applying [24, Lemma 4.3] there exists a constant $C_* > 0$ for the kernel $\frac{\gamma_*}{||\mathbf{x}-\mathbf{y}||^{d+2s}} \chi_{B_\varepsilon(\mathbf{x})}(\mathbf{y})$, s.t.

$$
C_*||u||_{L^2(\Omega)} \leq \iint\limits_{(\Omega \cup \Omega_I)^2} \frac{1}{2}(u(\mathbf{x}) - u(\mathbf{y}))^2 \frac{\gamma_*}{||\mathbf{x} - \mathbf{y}||_2^{d+2s}} \chi_{B_\varepsilon(\mathbf{x})}(\mathbf{y}) \, d\mathbf{y}d\mathbf{x}
$$

$$
= \iint\limits_{(\mathbf{F_t}(\Omega) \cup \Omega_I)^2} \frac{1}{2}(u(\mathbf{x}) - u(\mathbf{y}))^2 \frac{\gamma_*}{||\mathbf{x} - \mathbf{y}||_2^{d+2s}} \chi_{B_\varepsilon(\mathbf{x})}(\mathbf{y}) \, d\mathbf{y}d\mathbf{x}
$$

$$
\leq \iint\limits_{(\mathbf{F_t}(\Omega) \cup \Omega_I)^2} \frac{1}{2}(u(\mathbf{x}) - u(\mathbf{y}))^2 \gamma(\mathbf{x}, \mathbf{y}) \chi_{B_\varepsilon(\mathbf{x})}(\mathbf{y}) \, d\mathbf{y}d\mathbf{x} = A_{\Gamma^t}(u, u)
$$

So we conclude

$$
C_* ||u \circ \mathbf{F_t}^{-1}||_{L^2(\Omega)}^2 \leq A_{\Gamma^t}(u \circ \mathbf{F_t}^{-1}, u \circ \mathbf{F_t}^{-1}) = A(t, u, u).
$$

Since T is chosen small enough, $[0, T] \times \bar{\Omega}$ is a compact set and ξ^t is continuous on $[0, T] \times \bar{\Omega}$, there exists $\xi_* > 0$, s.t. $\xi^t(\mathbf{x}) \geq \xi_*$ for every $t \in [0, T]$ and $\mathbf{x} \in \bar{\Omega}$. Therefore, by using that $\mathbf{F_t}(\Omega) = \Omega$, we derive

$$
||u \circ \mathbf{F_t}^{-1}||_{L^2(\Omega)}^2 = \int_\Omega (u \circ \mathbf{F_t}^{-1})^2 \, d\mathbf{x} = \int_{\mathbf{F_t}(\Omega)} (u \circ \mathbf{F_t}^{-1})^2 \, d\mathbf{x}
$$

$$
= \int_\Omega u^2 \xi^t \, d\mathbf{x} \geq \xi_* \int_\Omega u^2 \, d\mathbf{x} = \xi_* ||u||_{L^2(\Omega)}^2.
$$

$\square$

In the following we prove that assumption (P1) also holds for a standard example of a singular symmetric kernel.

Example 4.5 For $\gamma(\mathbf{x}, \mathbf{y}) = \frac{\sigma(\mathbf{x}, \mathbf{y})}{||\mathbf{x}-\mathbf{y}||^{d+2s}} \chi_{B_\varepsilon(\mathbf{x})}(\mathbf{y})$ of Example 2.1, where additionally there exists a constant $\sigma^* \in (0, \infty)$ with $|\nabla_{\mathbf{x}}\sigma|, |\nabla_{\mathbf{y}}\sigma| \leq \sigma^*$, the assumption (P1) holds, since $\Omega \cup \Omega_I$ is a bounded domain and

$$
|\nabla_{\mathbf{x}}\gamma(\mathbf{x}, \mathbf{y})^\top \mathbf{V}(\mathbf{x}) + \nabla_{\mathbf{y}}\gamma(\mathbf{x}, \mathbf{y})^\top \mathbf{V}(\mathbf{y})|||\mathbf{x} - \mathbf{y}||_2^{d+2s}
$$

$$
\leq |\sigma(\mathbf{x}, \mathbf{y}) \frac{(\mathbf{x} - \mathbf{y})^\top (\mathbf{V}(\mathbf{x}) - \mathbf{V}(\mathbf{y}))}{||\mathbf{x} - \mathbf{y}||_2^2}| + |\nabla_{\mathbf{x}}\sigma(\mathbf{x}, \mathbf{y})^\top \mathbf{V}(\mathbf{x}) + \nabla_{\mathbf{y}}\sigma(\mathbf{x}, \mathbf{y})^\top \mathbf{V}(\mathbf{y})|
$$

$$
\leq L\gamma^* + 2\sigma^* \mathbf{V}^* < \infty,
$$

where we used that $\mathbf{V} \in C_0^1(\Omega \cup \Omega_I, \mathbb{R}^d)$ is Lipschitz continuous for some Lipschitz constant $L > 0$ and that there exists a $\mathbf{V}^* > 0$ with $|\mathbf{V}(\mathbf{x})| \leq \mathbf{V}^*$ for $\mathbf{x} \in \Omega \cup \Omega_I$.

Now we can show, that the additional requirements of AAM are satisfied by problem (12):

Lemma 4.6 *Let G be defined as in (17) and let the assumptions (P0) and (P1) be fulfilled. Then the assumptions (H0) and (H1) are satisfied and for every $t \in [0, T]$ there exists a solution $v^t \in V_c(\Omega \cup \Omega_I)$ that solves the averaged adjoint equation (18).*

Proof Because of the length of the proof, we move it to Appendix A. □

As a direct consequence of Theorem 3.2 and Lemma 4.6 we can state the next Corollary.

Corollary 4.7 *Let G be defined as in (17) and (P0) and (P1) be fulfilled. Then the reduced cost functional of (12) is shape differentiable and the shape derivative of the reduced cost functional can be expressed as*

$$D_\Gamma J^{red}(\Omega)[\mathbf{V}] = \partial_t G(0, u^0, v^0),$$

where u^0 is the solution to the state equation (11) and v^0 the solution to the adjoint equation (19).

The missing piece to implement the respective algorithmic realization presented in Section 3.3 is the shape derivative of the reduced objective functional, which is used in
Line 7 of Algorithm 1 and given by

$$D_\Gamma J^{red}(\Gamma)[\mathbf{V}] = \partial_t G(0, u^0, v^0) = \left.\frac{d}{dt}\right|_{t=0^+} J(t, u^0) + \left.\frac{d}{dt}\right|_{t=0^+}$$
$$A(t, u^0, v^0) - \left.\frac{d}{dt}\right|_{t=0^+} F(t, v^0). \tag{25}$$

As a first step, we formulate the shape derivative of the objective functional J and the linear functional F, which can also be found in the standard literature.

Theorem 4.8 (Shape derivative of the reduced objective functional) *Let the assumptions (P0) and (P1) be satisfied. Further let Γ be a shape with corresponding state variable u^0 and adjoint variable v^0. Then, for a vector field $\mathbf{V} \in C_0^1(\Omega \cup \Omega_I, \mathbb{R}^d)$ we find*

$$D_\Gamma J^{red}(\Gamma)[\mathbf{V}] = \int_\Omega -(u^0 - \bar{u})\nabla\bar{u}^\top\mathbf{V} + (u^0 - \bar{u})^2 \operatorname{div}\mathbf{V} \, d\mathbf{x}$$
$$+ \nu \int_\Gamma \operatorname{div}\mathbf{V} - \mathbf{n}^\top\nabla\mathbf{V}^\top\mathbf{n} \, ds \tag{26}$$
$$- \int_\Omega D_m f_\Gamma v^0 + \operatorname{div}\mathbf{V}(f v^0) \, d\mathbf{x} + D_\Gamma A_\Gamma(u^0, v^0)[\mathbf{V}].$$

Proof In order to prove this theorem, we just have to compute the shape derivative of the objective function $J(u^0, \Gamma)$ and of the linear functional $F_\Gamma(v^0)$. Therefore, let $\xi^t(\mathbf{x}) := \det D\mathbf{F_t}(\mathbf{x})$.

Then, we have $\xi^0(x) = \det D\mathbf{F_0}(\mathbf{x}) = \det(\mathbf{I}) = 1$ and $\frac{d}{dt}\big|_{t=0^+}\xi^t = \operatorname{div}\mathbf{V}$(see, e.g., [45]), such that the shape derivative of the right-hand side F_Γ can be derived as a consequence of [56, Proposition 2.32] and the product rule of Fréchet derivatives as follows

$$
D_\Gamma F_\Gamma(v^0)[\mathbf{V}] = \frac{d}{dt}\Big|_{t=0^+} F_{\Gamma^t}(v^0 \circ \mathbf{F_t}^{-1}) = \int_\Omega \frac{d}{dt}\Big|_{t=0^+} (f_\Gamma \circ \mathbf{F_t})v^0\xi^t\,dx
$$
$$
= \int_\Omega D_m f_\Gamma v^0\,dx + \int_\Omega f_\Gamma v^0\,\operatorname{div}\mathbf{V}\,dx.
$$

Moreover, the shape derivative of the objective functional can be written as

$$
D_\Gamma J(u^0, \Gamma)[\mathbf{V}] = D_\Gamma j(u^0, \Gamma)[\mathbf{V}] + D_\Gamma j_{reg}(\Gamma)[\mathbf{V}] = \frac{d}{dt}\Big|_{t=0^+} j(u^0 \circ \mathbf{F_t}^{-1}, \Gamma^t)
$$
$$
+ \frac{d}{dt}\Big|_{t=0^+} j_{reg}(\Gamma^t).
$$

Here the shape derivative of the regularization term is an immediate consequence of [62, Theorem 4.13] and is given by

$$
D_\Gamma j_{reg}(u^0, \Gamma)[\mathbf{V}] = \nu \int_\Gamma \operatorname{div}_\Gamma \mathbf{V}\,ds = \nu \int_\Gamma \operatorname{div}\mathbf{V} - \mathbf{n}^\top\nabla\mathbf{V}^\top\mathbf{n}\,ds,
$$

where $\mathbf{n}$ denotes the outer normal of Ω_1. Additionally, we obtain for the shape derivative of the tracking-type functional

$$
D_\Gamma j(u^0, \Gamma)[\mathbf{V}] = \frac{d}{dt}\Big|_{t=0^+} j(u^0 \circ \mathbf{F_t}^{-1}, \Gamma^t) = \frac{1}{2}\frac{d}{dt}\Big|_{t=0^+} \int_{\mathbf{F_t}(\Omega)} (u^0 \circ \mathbf{F_t}^{-1} - \bar{u})^2\,dx
$$
$$
= \frac{1}{2}\int_\Omega \frac{d}{dt}\Big|_{t=0^+} (u^0 - \bar{u}\circ \mathbf{F_t})^2\xi^t\,dx
$$
$$
= \int_\Omega -(u^0 - \bar{u})\nabla\bar{u}^\top\mathbf{V} + (u^0 - \bar{u})^2\,\operatorname{div}\mathbf{V}\,dx.
$$

Putting the above terms into equation (25) yields the formula of Theorem 4.8. □

The last step to derive the shape derivative of the reduced objective functional (25) is to compute the shape derivative of the nonlocal bilinear form A_Γ.

Lemma 4.9 (Shape derivative of the nonlocal bilinear form) *Let the assumptions (P0) and (P1) be satisfied. Further let Γ be a shape with corresponding state variable u^0*

and adjoint variable v^0. Then for a vector field $\mathbf{V} \in C_0^1(\Omega \cup \Omega_I, \mathbb{R}^d)$ we find for a square integrable kernel γ that

$$
\begin{aligned}
&\frac{d}{dt}\Big|_{t=0+} A(t, u^0, v^0) = D_\Gamma A_\Gamma(u^0, v^0)[\mathbf{V}] \\
&= \sum_{i,j=1,2} \int_{\Omega_i} \int_{\Omega_j} \left(v^0(\mathbf{x}) - v^0(\mathbf{y})\right) \left(u^0(\mathbf{x}) \nabla_x \gamma_{ij}(\mathbf{x}, \mathbf{y}) - u^0(\mathbf{y}) \nabla_y \gamma_{ji}(\mathbf{y}, \mathbf{x})\right)^\top \mathbf{V}(\mathbf{x}) \\
&\quad + (v^0(\mathbf{x}) - v^0(\mathbf{y}))(u^0(\mathbf{x})\gamma_{ij}(\mathbf{x}, \mathbf{y}) - u^0(\mathbf{y})\gamma_{ji}(\mathbf{y}, \mathbf{x}))\, \mathrm{div}\,\mathbf{V}(\mathbf{x})\, d\mathbf{y}d\mathbf{x} \\
&\quad + \sum_{i=1,2} \int_{\Omega_i} \int_{\Omega_I} u^0(\mathbf{x})v^0(\mathbf{x}) \nabla_x \gamma_{iI}(\mathbf{x}, \mathbf{y})^\top \mathbf{V}(\mathbf{x}) + u^0(\mathbf{x})v^0(\mathbf{x})\gamma_{iI}(\mathbf{x}, \mathbf{y})\, \mathrm{div}\,\mathbf{V}(\mathbf{x})\, d\mathbf{y}d\mathbf{x}.
\end{aligned}
$$

$$(27)$$

and for a singular kernel γ that

$$
\begin{aligned}
&D_\Gamma A_\Gamma(u^0, v^0)[\mathbf{V}] \\
&= \sum_{i,j=1,2} \frac{1}{2} \int_{\Omega_i} \int_{\Omega_j} (u^0(\mathbf{x}) - u^0(\mathbf{y}))(v^0(\mathbf{x}) \\
&\quad - v^0(\mathbf{y})) \left(\nabla_{\mathbf{x}} \gamma_{ij}(\mathbf{x}, \mathbf{y})^\top \mathbf{V}(\mathbf{x}) + \nabla_{\mathbf{y}} \gamma_{ij}(\mathbf{x}, \mathbf{y})^\top \mathbf{V}(\mathbf{y})\right)\, d\mathbf{y}d\mathbf{x} \\
&\quad + \sum_{i,j=1,2} \int_{\Omega_i} \int_{\Omega_j} (u^0(\mathbf{x}) - u^0(\mathbf{y}))(v^0(\mathbf{x}) - v^0(\mathbf{y}))\gamma_{ij}(\mathbf{x}, \mathbf{y})\, \mathrm{div}\,\mathbf{V}(\mathbf{x})\, d\mathbf{y}d\mathbf{x} \\
&\quad + \sum_{i=1,2} \int_{\Omega_i} \int_{\Omega_I} (u^0(\mathbf{x}) - u^0(\mathbf{y}))(v^0(\mathbf{x}) \\
&\quad - v^0(\mathbf{y})) \left(\nabla_{\mathbf{x}} \gamma_{iI}(\mathbf{x}, \mathbf{y})^\top \mathbf{V}(\mathbf{x}) + \gamma_{iI}(\mathbf{x}, \mathbf{y})\, \mathrm{div}\,\mathbf{V}(\mathbf{x})\right)\, d\mathbf{y}d\mathbf{x}.
\end{aligned}
$$

Proof Define $\xi^t(\mathbf{x}) := \det D\mathbf{F}_t(\mathbf{x})$ and $\gamma_{ij}^t(\mathbf{x}, \mathbf{y}) := \gamma_{ij}(\mathbf{F}_t(\mathbf{x}), \mathbf{F}_t(\mathbf{y}))$.

Case 1: Square integrable kernels

Then, we can write by using representation (8) of the nonlocal bilinear form A

$$
\begin{aligned}
&A(t, u^0, v^0) = A_{\Gamma^t}(u^0 \circ \mathbf{F}_t^{-1}, v^0 \circ \mathbf{F}_t^{-1}) \\
&= \frac{1}{2} \sum_{i,j=1,2} \int_{\Omega_i} \int_{\Omega_j} \left(v^0(\mathbf{x}) - v^0(\mathbf{y})\right) \left(u^0(\mathbf{x})\gamma_{ij}^t(\mathbf{x}, \mathbf{y}) - u^0(\mathbf{y})\gamma_{ji}^t(\mathbf{y}, \mathbf{x})\right) \\
&\quad \xi^t(\mathbf{x})\xi^t(\mathbf{y})\, d\mathbf{y}d\mathbf{x} \\
&\quad + \sum_{i=1,2} \int_{\Omega_i} \int_{\Omega_I} u^0(\mathbf{x})v^0(\mathbf{x})\gamma_{iI}(\mathbf{F}_t(\mathbf{x}), \mathbf{y})\xi^t(\mathbf{x})\, d\mathbf{y}d\mathbf{x}.
\end{aligned}
$$

First, we recall that the function ξ^t is continuously differentiable and $\frac{d}{dt}\big|_{t=0} \xi^t(\mathbf{x}) = div\,\mathbf{V}(\mathbf{x})$, see, e.g., [45].

So we derive the shape derivative of the nonlocal bilinear form by applying Lemma 4.1, as described in Remark 4.2, on $\gamma_{ij} \in W^{1,1}(\Omega \times \Omega, \mathbb{R})$ and $\gamma_{iI} \in W^{1,1}(\Omega \times \Omega_I, \mathbb{R})$ and by using the product rule for Fréchet derivatives

$$
\begin{aligned}
&\frac{d}{dt}\Big|_{t=0^+} A(t, u^0, v^0)\\
&= \frac{1}{2} \sum_{i,j=1,2} \int_{\Omega_i} \int_{\Omega_j} \left(v^0(\mathbf{x}) - v^0(\mathbf{y})\right) \left(u^0(\mathbf{x})\nabla_x \gamma_{ij}(\mathbf{x},\mathbf{y}) - u^0(\mathbf{y})\nabla_y \gamma_{ji}(\mathbf{y},\mathbf{x})\right)^\top \mathbf{V}(\mathbf{x})\\
&\quad + \left(v^0(\mathbf{x}) - v^0(\mathbf{y})\right) \left(u^0(\mathbf{x})\nabla_y \gamma_{ij}(\mathbf{x},\mathbf{y}) - u^0(\mathbf{y})\nabla_x \gamma_{ji}(\mathbf{y},\mathbf{x})\right)^\top \mathbf{V}(\mathbf{y})\\
&\quad + (v^0(\mathbf{x}) - v^0(\mathbf{y}))(u^0(\mathbf{x})\gamma_{ij}(\mathbf{x},\mathbf{y}) - u^0(\mathbf{y})\gamma_{ji}(\mathbf{y},\mathbf{x}))(\operatorname{div}\mathbf{V}(\mathbf{x}) + \operatorname{div}\mathbf{V}(\mathbf{y}))\,d\mathbf{y}d\mathbf{x}\\
&\quad + \sum_{i=1,2} \int_{\Omega_i}\int_{\Omega_I} u^0(\mathbf{x})v^0(\mathbf{x})\nabla_x \gamma_{iI}(\mathbf{x},\mathbf{y})^\top \mathbf{V}(\mathbf{x}) + u^0(\mathbf{x})v^0(\mathbf{x})\gamma_{iI}(\mathbf{x},\mathbf{y})\operatorname{div}\mathbf{V}(\mathbf{x})\,d\mathbf{y}d\mathbf{x}\\
&= \sum_{i,j=1,2} \int_{\Omega_i}\int_{\Omega_j} \left(v^0(\mathbf{x}) - v^0(\mathbf{y})\right) \left(u^0(\mathbf{x})\nabla_x \gamma_{ij}(\mathbf{x},\mathbf{y}) - u^0(\mathbf{y})\nabla_y \gamma_{ji}(\mathbf{y},\mathbf{x})\right)^\top \mathbf{V}(\mathbf{x})\\
&\quad + (v^0(\mathbf{x}) - v^0(\mathbf{y}))(u^0(\mathbf{x})\gamma_{ij}(\mathbf{x},\mathbf{y}) - u^0(\mathbf{y})\gamma_{ji}(\mathbf{y},\mathbf{x}))\operatorname{div}\mathbf{V}(\mathbf{x})\,d\mathbf{y}d\mathbf{x}\\
&\quad + \sum_{i=1,2} \int_{\Omega_i}\int_{\Omega_I} u^0(\mathbf{x})v^0(\mathbf{x})\nabla_x \gamma_{iI}(\mathbf{x},\mathbf{y})^\top \mathbf{V}(\mathbf{x}) + u^0(\mathbf{x})v^0(\mathbf{x})\gamma_{iI}(\mathbf{x},\mathbf{y})\operatorname{div}\mathbf{V}(\mathbf{x})\,d\mathbf{y}d\mathbf{x}.
\end{aligned}
$$

For the second equation, the following computations are used, which can be obtained by applying Fubini's theorem and by swapping $\mathbf{x}$ and $\mathbf{y}$

$$
\begin{aligned}
&\int_{\Omega_i}\int_{\Omega_j} (v^0(\mathbf{x}) - v^0(\mathbf{y}))(-u^0(\mathbf{y})\nabla_x \gamma_{ji}(\mathbf{y},\mathbf{x})^\top \mathbf{V}(\mathbf{y}))\,d\mathbf{y}d\mathbf{x}\\
&= \int_{\Omega_j}\int_{\Omega_i} (v^0(\mathbf{x}) - v^0(\mathbf{y}))(u^0(\mathbf{x})\nabla_x \gamma_{ji}(\mathbf{x},\mathbf{y})^\top \mathbf{V}(\mathbf{x}))\,d\mathbf{y}d\mathbf{x},\\[6pt]
&\int_{\Omega_i}\int_{\Omega_j} (v^0(\mathbf{x}) - v^0(\mathbf{y}))u^0(\mathbf{x})\nabla_y \gamma_{ij}(\mathbf{x},\mathbf{y})^\top \mathbf{V}(\mathbf{y})\,d\mathbf{y}d\mathbf{x}\\
&= -\int_{\Omega_j}\int_{\Omega_i} (v^0(\mathbf{x}) - v^0(\mathbf{y}))u^0(\mathbf{y})\nabla_y \gamma_{ij}(\mathbf{y},\mathbf{x})^\top \mathbf{V}(\mathbf{x})\,d\mathbf{y}d\mathbf{x} \text{ and}
\end{aligned}
$$

$$
\begin{aligned}
&\int_{\Omega_i}\int_{\Omega_j} (v^0(\mathbf{x}) - v^0(\mathbf{y}))(u^0(\mathbf{x})\gamma_{ij}(\mathbf{x},\mathbf{y}) - u^0(\mathbf{y})\gamma_{ji}(\mathbf{y},\mathbf{x}))\operatorname{div}\mathbf{V}(\mathbf{y})\,d\mathbf{y}d\mathbf{x}\\
&= \int_{\Omega_j}\int_{\Omega_i} (v^0(\mathbf{x}) - v^0(\mathbf{y}))(u^0(\mathbf{x})\gamma_{ji}(\mathbf{x},\mathbf{y}) - u^0(\mathbf{y})\gamma_{ij}(\mathbf{y},\mathbf{x}))\operatorname{div}\mathbf{V}(\mathbf{x})\,d\mathbf{y}d\mathbf{x}.
\end{aligned}
$$

Case 2: Singular kernels

Since $\xi^t(\mathbf{x}) = det\, D\mathbf{F_t}(\mathbf{x})$ is continuous and therefore bounded on $\Omega \cup \Omega_I$, we get that the double integral

$$A(t, u^0, v^0) = \frac{1}{2} \iint\limits_{(\Omega \cup \Omega_I)^2} (u^0(\mathbf{x}) - u^0(\mathbf{y}))(v^0(\mathbf{x}) - v^0(\mathbf{y}))\gamma^t(\mathbf{x}, \mathbf{y})\xi^t(\mathbf{x})\xi^t(\mathbf{y})\, d\mathbf{y}d\mathbf{x}$$

is well-defined(see also Remark 4.3). Moreover since $\gamma^t \in W^{1,1}(D_n, \mathbb{R})$ we can conclude, as outlined in Remark 4.2, that the function γ^t is differentiable in $L^1(D_n, \mathbb{R})$ with

$$\frac{d}{dt}\bigg|_{t=0} \gamma^t(\mathbf{x}, \mathbf{y}) = \nabla_\mathbf{x}\gamma(\mathbf{x}, \mathbf{y})^\top \mathbf{V}(\mathbf{x}) + \nabla_\mathbf{y}\gamma(\mathbf{x}, \mathbf{y})^\top \mathbf{V}(\mathbf{y}).$$

Therefore, we follow
  for the singular symmetric kernel

$$\frac{d}{dt}\bigg|_{t=0} A(t, u^0, v^0) = \lim_{n\to\infty} \frac{d}{dt}\bigg|_{t=0} \frac{1}{2} \iint\limits_{D_n} (u^0(\mathbf{x}) - u^0(\mathbf{y}))(v^0(\mathbf{x})$$

$$- v^0(\mathbf{y}))\gamma^t(\mathbf{x}, \mathbf{y})\xi^t(\mathbf{x})\xi^t(\mathbf{y})\, d\mathbf{y}d\mathbf{x}$$

$$= \lim_{n\to\infty} \frac{1}{2} \iint\limits_{D_n} (u^0(\mathbf{x}) - u^0(\mathbf{y}))(v^0(\mathbf{x}) - v^0(\mathbf{y}))$$

$$\left(\nabla_\mathbf{x}\gamma(\mathbf{x}, \mathbf{y})^\top \mathbf{V}(\mathbf{x}) + \nabla_\mathbf{y}\gamma(\mathbf{x}, \mathbf{y})^\top \mathbf{V}(\mathbf{y})\right)\, d\mathbf{y}d\mathbf{x}$$

$$+ \lim_{n\to\infty} \frac{1}{2} \iint\limits_{D_n} (u^0(\mathbf{x}) - u^0(\mathbf{y}))(v^0(\mathbf{x}) - v^0(\mathbf{y}))\gamma(\mathbf{x}, \mathbf{y})\,(\mathrm{div}\,\mathbf{V}(\mathbf{x}) + \mathrm{div}\,\mathbf{V}(\mathbf{y}))\, d\mathbf{y}d\mathbf{x}$$

$$= \frac{1}{2} \iint\limits_{(\Omega \cup \Omega_I)^2} (u^0(\mathbf{x}) - u^0(\mathbf{y}))(v^0(\mathbf{x}) - v^0(\mathbf{y}))\left(\nabla_\mathbf{x}\gamma(\mathbf{x}, \mathbf{y})^\top \mathbf{V}(\mathbf{x}) + \nabla_\mathbf{y}\gamma(\mathbf{x}, \mathbf{y})^\top \mathbf{V}(\mathbf{y})\right)\, d\mathbf{y}d\mathbf{x}$$

$$+ \frac{1}{2} \iint\limits_{(\Omega \cup \Omega_I)^2} (u^0(\mathbf{x}) - u^0(\mathbf{y}))(v^0(\mathbf{x}) - v^0(\mathbf{y}))\gamma(\mathbf{x}, \mathbf{y})\,(\mathrm{div}\,\mathbf{V}(\mathbf{x}) + \mathrm{div}\,\mathbf{V}(\mathbf{y}))\, d\mathbf{y}d\mathbf{x}$$

$$= \sum_{i,j=1,2} \frac{1}{2} \int_{\Omega_i} \int_{\Omega_j} (u^0(\mathbf{x}) - u^0(\mathbf{y}))(v^0(\mathbf{x}) - v^0(\mathbf{y}))$$

$$\left(\nabla_\mathbf{x}\gamma_{ij}(\mathbf{x}, \mathbf{y})^\top \mathbf{V}(\mathbf{x}) + \nabla_\mathbf{y}\gamma_{ij}(\mathbf{x}, \mathbf{y})^\top \mathbf{V}(\mathbf{y})\right)\, d\mathbf{y}d\mathbf{x} \tag{28}$$

$$+ \sum_{i,j=1,2} \int_{\Omega_i} \int_{\Omega_j} (u^0(\mathbf{x}) - u^0(\mathbf{y}))(v^0(\mathbf{x}) - v^0(\mathbf{y}))\gamma_{ij}(\mathbf{x}, \mathbf{y})\,\mathrm{div}\,\mathbf{V}(\mathbf{x})\, d\mathbf{y}d\mathbf{x} \tag{29}$$

$$+ \sum_{i=1,2} \int_{\Omega_i} \int_{\Omega_I} (u^0(\mathbf{x}) - u^0(\mathbf{y}))(v^0(\mathbf{x}) - v^0(\mathbf{y}))$$

$$\left(\nabla_\mathbf{x}\gamma_{iI}(\mathbf{x}, \mathbf{y})^\top \mathbf{V}(\mathbf{x}) + \gamma_{iI}(\mathbf{x}, \mathbf{y})\,\mathrm{div}\,\mathbf{V}(\mathbf{x})\right)\, d\mathbf{y}d\mathbf{x}, \tag{30}$$

where the integrals (28)–(30) are also well-defined, since div $\mathbf{V}$ is bounded on Ω and Assumption (P1) yields the existence of derivatives $\nabla \gamma_{ij}$ and $\nabla \gamma_{iI}$ and of constants $0 \leq C_1, C_2 < \infty$ with

$$|\nabla_{\mathbf{x}} \gamma_{ij}(\mathbf{x}, \mathbf{y})^\top \mathbf{V}(\mathbf{x}) + \nabla_{\mathbf{y}} \gamma_{ij}(\mathbf{x}, \mathbf{y})^\top \mathbf{V}(\mathbf{y})| \leq \frac{C_1}{||\mathbf{x} - \mathbf{y}||_2^{d+2s}} \quad \text{for a.e. } (\mathbf{x}, \mathbf{y}) \in \Omega \times \Omega \text{ and}$$

$$|\nabla_{\mathbf{x}} \gamma_{iI}(\mathbf{x}, \mathbf{y})^\top \mathbf{V}(\mathbf{x})| \leq \frac{C_2}{||\mathbf{x} - \mathbf{y}||_2^{d+2s}} \quad \text{for a.e. } (\mathbf{x}, \mathbf{y}) \in \Omega \times \Omega_I.$$

$\square$

5 Numerical experiments

In this section, we want to put the above derived formula (26) for the shape derivative of the reduced objective functional into numerical practice. In the following numerical examples we test one singular symmetric and one nonsymmetric square integrable kernel. Specifically,

$$\gamma_\Gamma^{sym}(\mathbf{x}, \mathbf{y}) = \phi^{sym}(\mathbf{x}, \mathbf{y}) \chi_{B_\delta(\mathbf{x})}(\mathbf{y}),$$

where

$$\phi^{sym}(\mathbf{x}, \mathbf{y}) = \begin{cases} 100 d_\delta \frac{1}{||\mathbf{x}-\mathbf{y}||_2^{2+2s}} & \text{if } (\mathbf{x}, \mathbf{y}) \in \Omega_1 \times \Omega_1, \\ 1.0 d_\delta \frac{1}{||\mathbf{x}-\mathbf{y}||_2^{2+2s}} & \text{if } (\mathbf{x}, \mathbf{y}) \in \Omega_2 \times \Omega_2, \\ 10 d_\delta \frac{1}{||\mathbf{x}-\mathbf{y}||_2^{2+2s}} & \text{else,} \end{cases}$$

with with scaling constants $d_\delta := \frac{2-2s}{\pi \delta^{2-2s}}$ and

$$\gamma_\Gamma^{nonsym}(\mathbf{x}, \mathbf{y}) = \phi^{nonsym}(\mathbf{x}, \mathbf{y}) \chi_{B_\delta(\mathbf{x})}(\mathbf{y}),$$

where

$$\phi^{nonsym}(\mathbf{x}, \mathbf{y}) = \begin{cases} 5.0 c_\delta & \text{if } \mathbf{x} \in \Omega_1, \\ 3.0 c_\delta & \text{if } \mathbf{x} \in \Omega_2, \end{cases}$$

with scaling constants $c_\delta := \frac{1}{\delta^4}$. We truncate all kernel functions by $\| \cdot \|_2$-balls of radius $\delta = 0.1$ so that $\Omega \cup \Omega_I \subset [-\delta, 1 + \delta]^2$. As a right-hand side we choose a piecewise constant function

$$f_\Gamma(\mathbf{x}) = 100 \chi_{\Omega_1}(\mathbf{x}) - 10 \chi_{\Omega_2}(\mathbf{x}),$$

i.e., $f_1 = 100$ and $f_2 = -10$. We note that the nonsymmetric kernel γ^{nonsym} satisfies the conditions for the class of integrable kernels considered in [61], such that the corresponding nonlocal problem is well-posed and also assumptions (P0) and (P1) can easily be verified in this case. The symmetric kernel γ^{sym} is a special case of Example 2.1 and therefore the assumptions (P0) and (P1) are met. The well-posedness of the nonlocal problem regarding the singular kernel is shown in [24]. As a perimeter regularization we choose $\nu = 0.001$ and, since we only utilize $\mathbf{V}$ with supp$(\mathbf{V}) \cap \Gamma_k \neq \emptyset$, where Γ_k is the current interface in iteration k of Algorithm 1, we additionally assume that the nonlocal boundary has no direct influence on the shape derivative of the nonlocal bilinear form $D_\Gamma A_\Gamma$, such that for all $\mathbf{V} \in C_0^1(\Omega \cup \Omega_I, \mathbb{R}^2)$ with supp$(\mathbf{V}) \cap \Gamma_k \neq \emptyset$ we have for the square integrable kernel

$$
D_\Gamma A_\Gamma(u^0, v^0)[\mathbf{V}] = \sum_{i,j=1,2} \iint_{\Omega_i \times \Omega_j} \left(v^0(\mathbf{x}) - v^0(\mathbf{y}) \right)
$$

$$
\left(u^0(\mathbf{x}) \nabla_x \gamma_{ij}(\mathbf{x}, \mathbf{y}) - u^0(\mathbf{y}) \nabla_y \gamma_{ji}(\mathbf{y}, \mathbf{x}) \right)^\top \mathbf{V}(\mathbf{x}) + (v^0(\mathbf{x})
$$

$$
- v^0(\mathbf{y}))(u^0(\mathbf{x}) \gamma_{ij}(\mathbf{x}, \mathbf{y}) - u^0(\mathbf{y}) \gamma_{ji}(\mathbf{y}, \mathbf{x})) \operatorname{div} \mathbf{V}(\mathbf{x}) \, d\mathbf{y} d\mathbf{x}
$$

and for the singular symmetric kernel

$$
D_\Gamma A_\Gamma(u^0, v^0)[\mathbf{V}]
$$

$$
= \sum_{i,j=1,2} \iint_{\Omega_i \times \Omega_j} \frac{1}{2}(u^0(\mathbf{x}) - u^0(\mathbf{y}))(v^0(\mathbf{x}) - v^0(\mathbf{y}))
$$

$$
\left(\nabla_{\mathbf{x}} \gamma_{ij}(\mathbf{x}, \mathbf{y})^\top \mathbf{V}(\mathbf{x}) + \nabla_{\mathbf{y}} \gamma_{ij}(\mathbf{x}, \mathbf{y})^\top \mathbf{V}(\mathbf{y}) \right)
$$

$$
+ (u^0(\mathbf{x}) - u^0(\mathbf{y}))(v^0(\mathbf{x}) - v^0(\mathbf{y}))\gamma_{ij}(\mathbf{x}, \mathbf{y}) \operatorname{div} \mathbf{V}(\mathbf{x}) \, d\mathbf{y} d\mathbf{x}.
$$

In order to solve problem (12), we apply a finite element method, where we employ continuous piecewise linear basis functions on triangular grids for the discretization of the nonlocal constraint equation. In particular we use the free meshing software Gmsh [30] to construct the meshes and a customized version of the Python package nlfem [35] to assemble the stiffness matrices of the nonlocal state and adjoint equation as well as the load vector regarding the shape derivative $D_\Gamma A_\Gamma$. Moreover, to assemble the load vector of the state and adjoint equation and the shape derivatives $D_\Gamma J$ and $D_\Gamma F_\Gamma$, we employ the open-source finite element software FEniCS [1, 2]. For a detailed discussion on the assembly of the nonlocal stiffness matrix we refer to [22, 35]. Here we solely emphasize how to implement a subdomain–dependent kernel of type (3). During the mesh generation each triangle is labeled according to its subdomain affiliation. Thus, whenever we integrate over a pair of two triangles, we can read out the labels (i, j) and choose the corresponding kernel γ_{ij}.

The data $\bar{u}$ is generated as solution $u(\overline{\Gamma})$ of the constraint equation associated to a target shape $\overline{\Gamma}$. Thus the data is represented as a linear combination of basis functions from the finite element basis. For the interpolation task in Line 3 of Algorithm 1
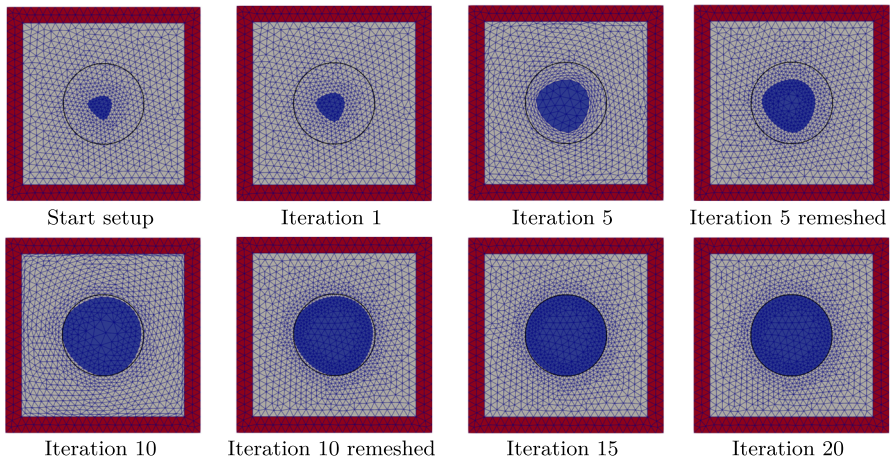
Fig. 2 Example 1 for the singular symmetric kernel
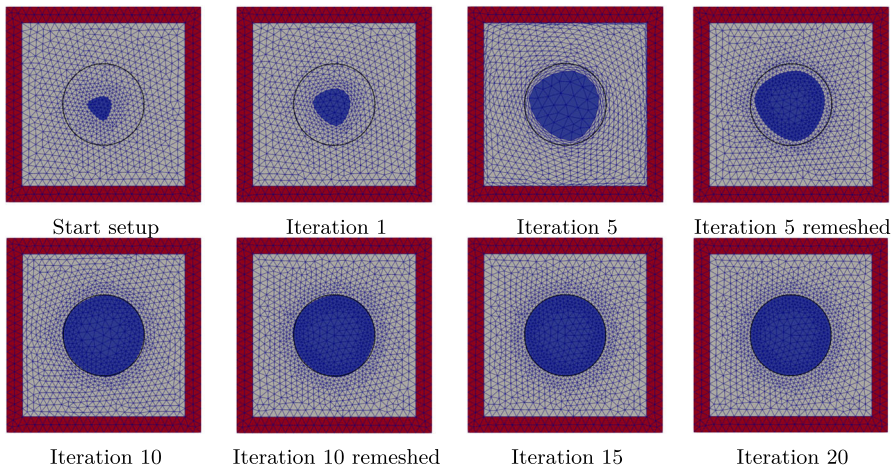
Fig. 3 Example 1 for the nonsymmetric integrable kernel

we solely need to translate between (non-matching) finite element grids by using the project function of FEniCS. In all examples below the target shape $\overline{\Gamma}$ is chosen to be a circle of radius 0.25 centered at (0.5, 0.5).

We now present two different non-trivial examples which differ in the choice of the initial guess Γ_0. They are presented and described in the Figs. 2 and 4 for the singular symmetric kernel and in the Figs. 3 and 5 for the nonsymmetric integrable kernel. In each plot of the aforementioned figures the black line represents the target interface $\overline{\Gamma}$. Moreover the blue area depicts Ω_1, the grey area Ω_2 and the red area the nonlocal interaction domain Ω_I.

Since the start shapes are smaller than the target shape, the shape needs to expand in the first few iterations. Thereby the nodes of the mesh are pushed towards the boundary, so that the mesh quality decreases and the algorithm stagnates, because
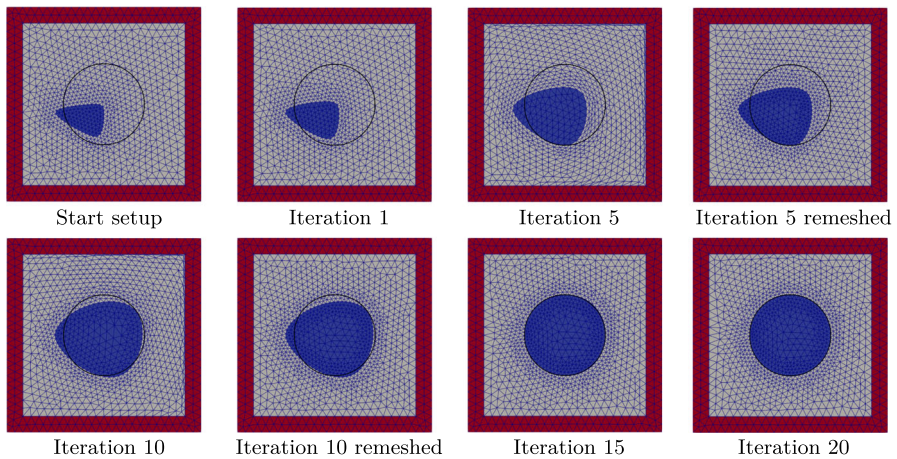
**Fig. 4** Example 2 for the singular symmetric kernel
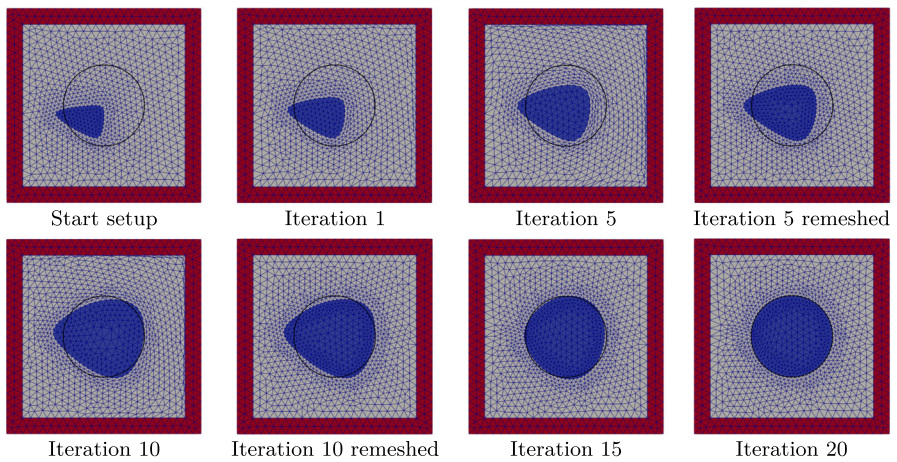
Fig. 5 Example 2 for the nonsymmetric integrable kernel

nodes are prohibited to be pushed outside of Ω. Therefore, we apply a remeshing technique, where we remesh after the fifth and tenth iteration. In order to remesh, we save the points of our current shape as a spline in a dummy.geo file, that also contains the information of the nonlocal boundary, and then compute a new mesh with Gmsh. In this new mesh the distance between the nodes and the boundary is sufficiently large to attain a better improvement regarding the objective function value by the new mesh deformations.

It is important to mention that computation times and the performance of Algorithm 1 in general are very sensitive to the choice of parameters and may strongly vary, which is why reporting exact computation times is not very meaningful at this stage. Particularly delicate choices are those of the system parameters including the kernel (diffusion and convection) and the forcing term, which both determine the identifia-
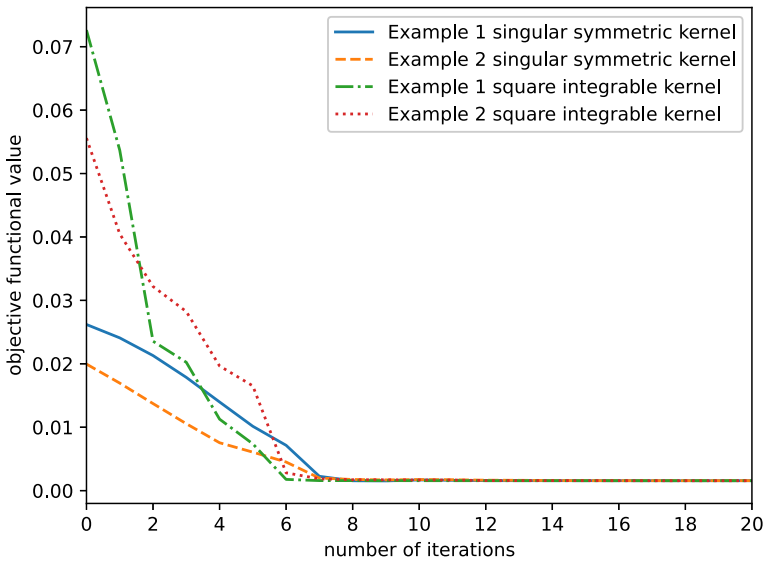
Fig. 6 In the first six or seven iterations the improvement regarding the objective function value is quite high. After that the objective function value decreases in a much slower fashion. Due to the regularization term the objective functional value will not converge to zero

bility of the model. But also the choice of Lamé parameters to control the step size, specifically μ_{max} (we set $\mu_{min} = 0$ in all experiments). The convergence history of each experiment is shown in Fig. 6.

Moreover, especially in the case of system parameters with high interface-sensitivity in combination with an inconveniently small μ_{max}, mesh deformations may be large in the early phase of the algorithm. Thus, such mesh deformations $\tilde{\mathbf{U}}_k$ of high magnitude lead to destroyed meshes so that an evaluation of the reduced objective functional $J^{red}((\mathbf{Id} + \alpha\tilde{\mathbf{U}}_k)(\Omega_k))$, which requires the assembly of the nonlocal stiffness matrix, becomes a pointless computation. In order to avoid such computations we first perform a line search depending on one simple mesh quality criterion. More precisely, we downscale the step size, i.e., $\alpha = \tau\alpha$, until all finite element nodes of the resulting mesh $(\mathbf{Id} + \alpha\tilde{\mathbf{U}}_k)(\Omega_k)$ are a subset of Ω. After that, we continue with the backtracking line search in Line 18 of Algorithm 1.

6 Concluding remarks and future work

We have conducted a numerical investigation of shape optimization problems which are constrained by nonlocal system models. We have proven through numerical experiments the applicability of established shape optimization techniques for which the shape derivative of the nonlocal bilinear form represents the novel ingredient. All in all, this work is only a first step along the exploration of the interesting field of nonlocally constrained shape optimization problems.

A Proof of Lemma 4.6

Proof Define $\bar{u}^t(\mathbf{x}) := \bar{u}(\mathbf{F_t}(\mathbf{x}))$, $\xi^t(\mathbf{x}) := \det D\mathbf{F_t}(\mathbf{x})$, $\gamma_\Gamma^t(\mathbf{x}, \mathbf{y}) := \gamma_\Gamma(\mathbf{F_t}(\mathbf{x}), \mathbf{F_t}(\mathbf{y}))$, $f_\Gamma^t(\mathbf{x}) := f_\Gamma(\mathbf{F_t}(\mathbf{x}))$ and $\nabla f_\Gamma^t(\mathbf{x}) := \nabla f_\Gamma(\mathbf{F_t}(\mathbf{x}))$.

Assumption(H0):

Set $\tilde{G} : [0, 1] \to \mathbb{R}$, $\tilde{G}(s) = G(t, su^t + (1-s)u^0, v)$. We show that $\tilde{G}$ is continuous differentiable and therefore also absolutely continuous. By using the linearity of A we can compute

$$
\begin{aligned}
\partial_s \tilde{G}(s) &= d_u G(t, su^t + (1-s)u^0, v)[u^t - u^0] \\
&= d_u A(t, su^t + (1-s)u^0, v)[u^t - u^0] + d_u J(t, su^t + (1-s)u^0)[u^t - u^0] \\
&= A(t, u^t - u^0, v) + \int_\Omega \left(su^t + (1-s)u^0 - \bar{u}^t \right) \left(u^t - u^0 \right) \xi^t \, d\mathbf{x} \\
&= A(t, u^t - u^0, v) + s \int_\Omega \left(u^t - u^0 \right)^2 \xi^t \, d\mathbf{x} + \int_\Omega \left(u^0 - \bar{u}^t \right) \left(u^t - u^0 \right) \xi^t \, d\mathbf{x},
\end{aligned}
$$

which is obviously continuous and therefore the first condition of Assumption (H0) holds.

Furthermore the second criterion of (H0) is also satisfied:

$$
\begin{aligned}
\int_0^1 &|d_u G(t, su^t + (1-s)u^0, v)[\tilde{u}]| \, ds \\
&= \int_0^1 |A(t, \tilde{u}, v) + \int_\Omega (su^t + (1-s)u^0 - \bar{u})\tilde{u}\xi^t \, d\mathbf{x}| ds \\
&\leq |A(t, \tilde{u}, v)| + \int_0^1 s \, ds| \int_\Omega (u^t - u^0)\tilde{u}\xi^t \, d\mathbf{x}| + |\int_\Omega (u^0 - \bar{u}^t)\tilde{u}\xi^t \, d\mathbf{x}| \\
&= |A(t, \tilde{u}, v)| + \frac{1}{2}| \int_\Omega (u^t - u^0)\tilde{u}\xi^t \, d\mathbf{x}| + |\int_\Omega (u^0 - \bar{u}^t)\tilde{u}\xi^t \, d\mathbf{x}| < \infty.
\end{aligned}
$$

As mentioned in Sect. 3.2 the averaged adjoint equation (18) can be reformulated as

$$
A(t, \tilde{u}, v^t) = -\int_\Omega \left(\frac{1}{2}(u^t + u^0) - \bar{u}^t \right) \tilde{u}\xi^t \, d\mathbf{x} \quad \text{for all } \tilde{u} \in V_c(\Omega \cup \Omega_I). \quad (31)
$$

Since the right hand side of (31) is a linear and continuous operator with regards to $\tilde{u}$, Eq. (31) is a well-defined nonlocal problem, which has a unique solution v^t due to the assumptions (P0). By further using assumptions (P0), we can conclude for u^t, that there exists a $C_2 > 0$, such that

$$
\begin{aligned}
||u^t||_{L^2(\Omega)}^2 &\leq C_1 |A(t, u^t, u^t)| = C_1 |(f^t \xi^t, u^t)_{L^2(\Omega)}| \leq C_1 ||f^t \xi^t||_{L^2(\Omega)} ||u^t||_{L^2(\Omega)} \\
&\Rightarrow ||u^t||_{L^2(\Omega)} \leq C_1 ||f^t \xi^t||_{L^2(\Omega)} \leq C_2,
\end{aligned}
$$

where we used in the last step, that $||f_\Gamma^t \xi^t||_{L^2(\Omega)} \to ||f_\Gamma||_{L^2(\Omega)}$ ([58, Lemma 2.16]). Since $\xi^t(\mathbf{x}) = \det(\mathbf{I} + t D\mathbf{V}(\mathbf{x}))$ is continuous on $[0, T] \times \bar{\Omega}$, there exists a $\bar{\xi}$, such

that $|\xi^t(\mathbf{x})| \leq \bar{\xi}$ for all $(t, \mathbf{x}) \in [0, T] \times \bar{\Omega}$. Because $\bar{u}^t \to \bar{u}$ in $L^2(\Omega)$, there exists a $C_3 > 0$ with $||\bar{u}^t||_2 < C_3$ for $t \in [0, T]$. Then we derive for v^t that

$$
\begin{aligned}
||v^t||^2_{L^2(\Omega)} &\leq C_1|A(t, v^t, v^t)| = C_1|(\frac{1}{2}(u^t + u^0) - \bar{u}^t)\xi^t, v^t)_{L^2(\Omega)}| \\
&\leq \bar{\xi}C_1||\frac{1}{2}(u^t + u^0) - \bar{u}^t||_{L^2(\Omega)}||v^t||_{L^2(\Omega)} \\
\Rightarrow ||v^t||_{L^2(\Omega)} &\leq \bar{\xi}C_1||\frac{1}{2}(u^t + u^0) - \bar{u}^t||_{L^2(\Omega)} \leq \bar{\xi}C_1||\bar{u}^t||_{L^2(\Omega)} \\
&\quad + \frac{1}{2}\bar{\xi}C_1(||u^t||_{L^2(\Omega)} + ||u^0||_{L^2(\Omega)}) \\
&\leq \bar{\xi}C_1C_3 + \bar{\xi}C_1C_2.
\end{aligned}
$$

Assumption (H1):
Since u^t and v^t are bounded for $t \in [0, T]$, then for every sequence $\{t_n\}_{n\in\mathbb{N}}$ with $t_n \to 0$ there exist subsequences $\{t_{n_k}\}_{k\in\mathbb{N}}$ and $\{t_{n_l}\}_{l\in\mathbb{N}}$, such that there exist functions $q_1, q_2 \in L^2(\Omega \cup \Omega_I)$ with $u^{t_{n_l}} \rightharpoonup q_1$ $v^{t_{n_k}} \rightharpoonup q_2$ in $L^2(\Omega \cup \Omega_I)$.

In the next part of the proof, we will make use of the following observation: Let $\{t_k\}_{k\in\mathbb{N}} \in [0, T]^\mathbb{N}$ be a sequence with $t_k \to 0$ for $k \to \infty$ and $g^t, h^{t_k}, h^0 \in L^2(\Omega \cup \Omega_I)$ for $t \in [0, T]$ and $k \in \mathbb{N}$. Additionally, assume that $g^t \to g^0$ and $h^{t_k} \rightharpoonup h^0$ in $L^2(\Omega \cup \Omega_I)$ holds. Then, we can conclude

$$
\left|\int_\Omega h^{t_k} g^t \, d\mathbf{x} - \int_\Omega h^0 g^0 \, d\mathbf{x}\right| \leq \left|\int_\Omega h^{t_k}(g^t - g^0) \, d\mathbf{x}\right| + \left|\int_\Omega (h^{t_k} - h^0)g^0 \, d\mathbf{x}\right|
$$
$$
\leq ||h^{t_k}||_{L^2(\Omega)}||g^t - g^0||_{L^2(\Omega)} + |\int_\Omega (h^{t_k} - h^0)g^0 \, d\mathbf{x}| \to 0 \text{ for } k \to \infty \text{ and } t \searrow 0.
$$
(32)

Case 1: Proof of (H1) for square integrable kernels
Since ϕ_{ij} is essentially bounded on $\Omega \times \Omega$, ϕ_{iI} is essentially bounded on $\Omega \times \Omega_I$ and ξ^t is continuous and therefore bounded on $\bar{\Omega}$, we can conclude that

$$
\psi_t(\mathbf{y}) := (v(\mathbf{x}) - v(\mathbf{y}))\gamma_\Gamma^t(\mathbf{x}, \mathbf{y})\xi^t(\mathbf{x})\xi^t(\mathbf{y}) \in L^2(\Omega \cup \Omega_I)
$$

Then, applying [58, Lemma 2.16] yields $\gamma^t \to \gamma$ in $L^2(\Omega \times (\Omega \cup \Omega_I))$ and therefore $\gamma^t(\mathbf{x}, \mathbf{y}) \to \gamma(\mathbf{x}, \mathbf{y})$ for a.e. $(\mathbf{x}, \mathbf{y}) \in \Omega \times (\Omega \cup \Omega_I)$. As a consequence by using the dominated convergence theorem we get

$$
\psi_t(\mathbf{y}) \to (v(\mathbf{x}) - v(\mathbf{y}))\gamma_\Gamma(\mathbf{x}, \mathbf{y}) \text{ in } L^2(\Omega \cup \Omega_I) \text{ for } t \searrow 0.
$$

Thus, by (32) we derive

$$
\int_\Omega (v(\mathbf{x}) - v(\mathbf{y}))(u^{t_{n_l}}(\mathbf{x})\gamma_\Gamma^{t_{n_l}}(\mathbf{x}, \mathbf{y}) - u^{t_{n_l}}(\mathbf{y})\gamma_\Gamma^{t_{n_l}}(\mathbf{y}, \mathbf{x}))\xi^{t_{n_l}}(\mathbf{x})\xi^{t_{n_l}}(\mathbf{y}) \, d\mathbf{y}
$$
$$
\to \int_\Omega (v(\mathbf{x}) - v(\mathbf{y}))(q_1(\mathbf{x})\gamma_\Gamma(\mathbf{x}, \mathbf{y}) - q_1(\mathbf{y})\gamma_\Gamma(\mathbf{y}, \mathbf{x})) \, d\mathbf{y} \text{ for } \mathbf{x} \in \Omega, v \in L_c^2(\Omega \cup \Omega_I).
$$

Due to the continuity of parameter integrals, we have

$$\int_\Omega \int_\Omega (v(\mathbf{x}) - v(\mathbf{y}))(u^{t_{n_l}}(\mathbf{x})\gamma_\Gamma^{t_{n_l}}(\mathbf{x},\mathbf{y}) - u^{t_{n_l}}(\mathbf{y})\gamma_\Gamma^{t_{n_l}}(\mathbf{y},\mathbf{x}))\xi^{t_{n_l}}(\mathbf{x})\xi^{t_{n_l}}(\mathbf{y})\, d\mathbf{y}d\mathbf{x}$$
$$\rightarrow \int_\Omega \int_\Omega (v(\mathbf{x}) - v(\mathbf{y}))(q_1(\mathbf{x})\gamma_\Gamma(\mathbf{x},\mathbf{y}) - q_1(\mathbf{y})\gamma_\Gamma(\mathbf{y},\mathbf{x}))\, d\mathbf{y}d\mathbf{x}.$$

Analogously, we can show

$$\int_\Omega u^{t_{n_l}}(\mathbf{x})v(\mathbf{x})\int_{\Omega_I} \gamma_\Gamma^{t_{n_l}}(\mathbf{x},\mathbf{y})\xi^{t_{n_l}}(\mathbf{x})\, d\mathbf{y}d\mathbf{x} \rightarrow \int_\Omega q_1(\mathbf{x})v(\mathbf{x})\int_{\Omega_I}\gamma_\Gamma(\mathbf{x},\mathbf{y})\, d\mathbf{y}d\mathbf{x}.$$

So we can conclude $\lim_{l\to\infty} A(t_{n_l}, u^{t_{n_l}}, v) = A(0, q_1, v)$. Because $f_\Gamma^t\xi^t \rightarrow f_\Gamma$ in $L^2(\Omega)$ according to [58, Lemma 2.16], we can compute for all $v \in L_c^2(\Omega \cup \Omega_I)$

$$A(0, q_1, v) = \lim_{l\to\infty} A(t_{n_l}, u^{t_{n_l}}, v) = \lim_{l\to\infty} \int_\Omega f_\Gamma^{t_{n_l}} v \xi^{t_{n_l}}\, d\mathbf{x} = \int_\Omega f_\Gamma v\, d\mathbf{x}.$$

Since the solution is unique we derive $q_1 = u^0$ and $u^t \rightharpoonup u^0$. Similarly, we have for q_2 and for all $\tilde{u} \in L_c^2(\Omega \cup \Omega_I)$

$$A(0, \tilde{u}, q_2) = \lim_{k\to\infty} A(t_{n_k}, \tilde{u}, v^{t_{n_k}}) = -\lim_{k\to\infty} \int_\Omega (\frac{1}{2}(u^{t_{n_k}} + u^0) - \bar{u}^{t_{n_k}})\tilde{u}\xi^{t_{n_k}}\, d\mathbf{x}$$
$$= -\int_\Omega (u^0 - \bar{u})\tilde{u}\, d\mathbf{x}.$$

So we conclude $q_2 = v^0$ and $v^t \rightharpoonup v^0 (t \searrow 0)$. By using the mean value theorem, there exist $s_t \in (0, t)$, s.t. $s_t \to 0 (t \searrow 0)$ and

$$\frac{G(t, u^0, v^t) - G(0, u^0, v^t)}{t} = \partial_t G(s_t, u^0, v^t).$$

Therefore we now prove assumption (H1) by showing

$$\lim_{s,t \searrow 0} \partial_t G(t, u^0, v^s) = \partial_t G(0, u^0, v^0).$$

Computing the derivative regarding t yields

$$\partial_t G(t, u^0, v^s) = \partial_t A(t, u^0, v^s) - \partial_t F(t, v^s) + \partial_t J(t, u^0).$$

First we can show

$$\partial_t F(t, v^s) = \int_\Omega (\nabla f_\Gamma^t)^\top \mathbf{V} v^s \xi^t\, d\mathbf{x} + \int_\Omega f_\Gamma^t v^s \frac{d}{dr}\Big|_{r=t^+} \xi^r\, d\mathbf{x}$$
$$\rightarrow \int_\Omega (\nabla f_\Gamma)^\top \mathbf{V} v^0\, d\mathbf{x} + \int_\Omega f_\Gamma v^0 \operatorname{div} \mathbf{V}\, d\mathbf{x} = \partial_t F(0, v^0) \text{ as follows:}$$

$$(33)$$

By applying [58, Lemma 2.16], we obtain $\nabla f_\Gamma^t \xi^t \to \nabla f_\Gamma$ in $L^2(\Omega, \mathbb{R}^d)$ and $f_\Gamma^t \to f_\Gamma$ in $L^2(\Omega)$. Since every $\mathbf{V} \in C_0^1(\Omega \cup \Omega_I, \mathbb{R}^d)$ is bounded, we can conclude $(\nabla f_\Gamma^t)^\top \mathbf{V} \xi^t \to \nabla f_\Gamma^\top \mathbf{V}$ in $L^2(\Omega)$. Moreover for every $t \in [0, T)$ the derivative $\frac{d}{dr}\big|_{r=t^+} \xi^r = \frac{d}{dr}\big|_{r=t^+} \det(I + rD\mathbf{V})$ is continuous in r and $\frac{d}{dr}\big|_{r=0^+} \xi^r = \operatorname{div} \mathbf{V}$(see e.g. [45]), so we derive $f_\Gamma^t \frac{d}{dr}\big|_{r=t^+} \xi^r \to f_\Gamma \operatorname{div} \mathbf{V}$ in $L^2(\Omega)$. Again by using (32), we obtain the convergence in (33).

Analogously, the convergence of $\lim_{t \searrow 0} \partial_t J(t, u^0) = \partial_t J(0, u^0)$ can be shown.

Furthermore, we now employ representation (7) of the nonlocal bilinear form A to compute the partial derivative of A regarding t

$$
\begin{aligned}
&\partial_t A(t, u^0, v^s) \\
&= \int_\Omega \int_{\Omega \cup \Omega_I} v^s(\mathbf{x}) \underbrace{\left(u^0(\mathbf{x})\nabla_{\mathbf{x}}\gamma_\Gamma^t(\mathbf{x}, \mathbf{y}) - u^0(\mathbf{y})\nabla_{\mathbf{y}}\gamma_\Gamma^t(\mathbf{y}, \mathbf{x})\right)^\top \mathbf{V}(\mathbf{x})\xi^t(\mathbf{x})\xi^t(\mathbf{y})}_{=:A_1(t,u^0)(\mathbf{x},\mathbf{y})} \, d\mathbf{y} d\mathbf{x} \\
&\quad + \int_\Omega \int_{\Omega \cup \Omega_I} v^s(\mathbf{x}) \underbrace{\left(u^0(\mathbf{x})\nabla_{\mathbf{y}}\gamma_\Gamma^t(\mathbf{x}, \mathbf{y}) - u^0(\mathbf{y})\nabla_{\mathbf{x}}\gamma_\Gamma^t(\mathbf{y}, \mathbf{x})\right)^\top \mathbf{V}(\mathbf{y})\xi^t(\mathbf{x})\xi^t(\mathbf{y})}_{A_2(t,u^0)(\mathbf{x},\mathbf{y})} \, d\mathbf{y} d\mathbf{x} \\
&\quad + \int_\Omega \int_{\Omega \cup \Omega_I} v^s(\mathbf{x}) \underbrace{\left(u^0(\mathbf{x})\gamma_\Gamma^t(\mathbf{x}, \mathbf{y}) - u^0(\mathbf{y})\gamma_\Gamma^t(\mathbf{y}, \mathbf{x})\right) \frac{d}{dr}\Big|_{r=t^+}\left(\xi^r(\mathbf{x})\xi^r(\mathbf{y})\right)}_{A_3(t,u^0)(\mathbf{x},\mathbf{y})} \, d\mathbf{y} d\mathbf{x}.
\end{aligned}
$$

Since $\frac{d}{dr}\big|_{r=t^+} \xi^r(\mathbf{x})$ and $\xi^t(\mathbf{x})$ are continuous in $\mathbf{x} \in \bar{\Omega}$, ϕ_{ij}, $\nabla \phi_{ij}$ are essentially bounded for $(\mathbf{x}, \mathbf{y}) \in \bar{\Omega} \times \bar{\Omega}$ and ϕ_{iI}, $\nabla \phi_{iI}$ are essentially bounded for $(\mathbf{x}, \mathbf{y}) \in \bar{\Omega} \times \bar{\Omega}_I$, we can conclude in the same manner as above that $A_i(t, u^0)(\mathbf{x}, \cdot) \in L^2(\Omega \cup \Omega_I)$ for all $\mathbf{x} \in \Omega \setminus \Gamma$ and therefore

$$
\begin{aligned}
&\int_\Omega \int_{\Omega \cup \Omega_I} v^s(\mathbf{x}) A_i(t, u^0)(\mathbf{x}, \mathbf{y}) \, d\mathbf{y} d\mathbf{x} \\
&\to \int_\Omega \int_{\Omega \cup \Omega_I} v^0(\mathbf{x}) A_i(0, u^0)(\mathbf{x}, \mathbf{y}) \, d\mathbf{y} d\mathbf{x} \quad (i = 1, 2, 3).
\end{aligned}
$$

As a consequence, we derive $\lim_{s,t \searrow 0} \partial_t A(t, u^0, v^s) = \partial_t A(0, u^0, v^0)$.

All in all, we obtain

$$
\begin{aligned}
\lim_{s,t \searrow 0} \partial_t G(t, u^0, v^s) &= \lim_{s,t \searrow 0} \partial_t A(t, u^0, v^s) - \lim_{s,t \searrow 0} \partial_t F(t, v^s) + \lim_{t \searrow 0} \partial_t J(t, u^0) \\
&= \partial_t A(0, u^0, v^0) - \partial_t F(0, v^0) + \partial_t J(0, u^0) = \partial_t G(0, u^0, v^0).
\end{aligned}
$$

Case 2: Proof of (H1) for singular kernels

Define $D_n := \{(x, y) \in (\Omega \cup \Omega_I)^2 : ||\mathbf{x} - \mathbf{y}||_2 > \frac{1}{n}\}$ for $n \in \mathbb{N}$. Since, as shown in Remark 4.3, $\gamma^t(\mathbf{x}, \mathbf{y}) < L\gamma^* n^{d+2s}$ for all $t \in [0, T]$, $(x, y) \in D_n$ and ξ^t is continuous

on $\bar{\Omega} \cup \bar{\Omega}_I$, we can conclude that

$$\iint_{(\Omega \cup \Omega_I)^2} \left((v(\mathbf{x}) - v(\mathbf{y})) \gamma^{t_l}(\mathbf{x}, \mathbf{y}) \xi^{t_l}(\mathbf{x}) \xi^{t_l}(\mathbf{y}) \chi_{D_n}(\mathbf{x}, \mathbf{y}) \right)^2 \, d\mathbf{y} d\mathbf{x} < \infty$$

and by using [58, Lemma 2.16] that

$$\lim_{l \to \infty} \iint_{(\Omega \cup \Omega_I)^2} (v(\mathbf{x}) - v(\mathbf{y})) \gamma^{t_l}(\mathbf{x}, \mathbf{y}) \xi^{t_l}(\mathbf{x}) \xi^{t_l}(\mathbf{y}) \chi_{D_n}(\mathbf{x}, \mathbf{y}) \, d\mathbf{y} d\mathbf{x}$$

$$= \iint_{(\Omega \cup \Omega_I)^2} (v(\mathbf{x}) - v(\mathbf{y})) \gamma(\mathbf{x}, \mathbf{y}) \chi_{D_n^0}(\mathbf{x}, \mathbf{y}) \, d\mathbf{y} d\mathbf{x}.$$

With this convergence and (32), we derive the second step and with the dominated convergence theorem we get the first and third step of the following computation

$$\frac{1}{2} \iint_{(\Omega \cup \Omega_I)^2} (v(\mathbf{x}) - v(\mathbf{y}))(q_1(\mathbf{x}) - q_1(\mathbf{y})) \gamma(\mathbf{x}, \mathbf{y}) \, d\mathbf{y} d\mathbf{x}$$

$$= \lim_{n \to \infty} \frac{1}{2} \iint_{D_n} (v(\mathbf{x}) - v(\mathbf{y}))(q_1(\mathbf{x}) - q_1(\mathbf{y})) \gamma(\mathbf{x}, \mathbf{y}) \, d\mathbf{y} d\mathbf{x}$$

$$= \lim_{n \to \infty} \lim_{l \to \infty} \frac{1}{2} \iint_{D_n} (v(\mathbf{x}) - v(\mathbf{y}))(u^{t_l}(\mathbf{x}) - u^{t_l}(\mathbf{y})) \gamma^{t_l}(\mathbf{x}, \mathbf{y}) \xi^{t_l}(\mathbf{x}) \xi^{t_l}(\mathbf{y}) \, d\mathbf{y} d\mathbf{x}$$

$$= \lim_{l \to \infty} \frac{1}{2} \iint_{(\Omega \cup \Omega_I)^2} (v(\mathbf{x}) - v(\mathbf{y}))(u^{t_l}(\mathbf{x}) - u^{t_l}(\mathbf{y})) \gamma^{t_l}(\mathbf{x}, \mathbf{y}) \xi^{t_l}(\mathbf{x}) \xi^{t_l}(\mathbf{y}) \, d\mathbf{y} d\mathbf{x}$$

$$= \lim_{l \to \infty} \int_{\Omega} f^{t_l} v \xi^{t_l} \, d\mathbf{x} = \int_{\Omega} f v \, d\mathbf{x}.$$

So we can conclude, that $q_1 = u^0$ and $u^t \rightharpoonup u^0$. Analogously, we can show

$$\frac{1}{2} \iint_{(\Omega \cup \Omega_I)^2} (u(\mathbf{x}) - u(\mathbf{y}))(q_2(\mathbf{x}) - q_2(\mathbf{y})) \gamma(\mathbf{x}, \mathbf{y}) \, d\mathbf{y} d\mathbf{x}$$

$$= \lim_{n \to \infty} \frac{1}{2} \iint_{D_n} (u(\mathbf{x}) - u(\mathbf{y}))(q_2(\mathbf{x}) - q_2(\mathbf{y})) \gamma(\mathbf{x}, \mathbf{y}) \, d\mathbf{y} d\mathbf{x}$$

$$= \lim_{k \to \infty} \lim_{n \to \infty} \frac{1}{2} \iint_{D_n} (u(\mathbf{x}) - u(\mathbf{y}))(v^{t_k}(\mathbf{x}) - v^{t_k}(\mathbf{y})) \gamma^{t_k}(\mathbf{x}, \mathbf{y}) \xi^{t_k}(\mathbf{x}) \xi^{t_k}(\mathbf{y}) \, d\mathbf{y} d\mathbf{x}$$

$$= \lim_{k \to \infty} \frac{1}{2} \iint_{(\Omega \cup \Omega_I)^2} (u(\mathbf{x}) - u(\mathbf{y}))(v^{t_k}(\mathbf{x}) - v^{t_k}(\mathbf{y})) \gamma^{t_k}(\mathbf{x}, \mathbf{y}) \xi^{t_k}(\mathbf{x}) \xi^{t_k}(\mathbf{y}) \, d\mathbf{y} d\mathbf{x}$$

$$= -\lim_{k\to\infty} \int_\Omega \left(\frac{1}{2}(u^{t_k} + u^0) - \bar{u}^{t_k}\right) u\xi^{t_k}\, d\mathbf{y}d\mathbf{x} = -\int_\Omega (u^0 - \bar{u})u\, d\mathbf{x}$$

and therefore derive $q_2 = v^0$ and $v^t \rightharpoonup v^0$. As in case 1, the next step is to prove

$$\lim_{s,t\searrow 0} \partial_t G(t, u^0, v^s) = \partial_t G(0, u^0, v^0).$$

By again applying (32) and the dominated convergence theorem we conclude

$$\lim_{s,t\searrow 0} \partial_t A(t, u^0, v^s)$$

$$= \lim_{s,t\searrow 0} \frac{1}{2} \iint_{(\Omega\cup\Omega_I)^2} (v^s(\mathbf{x}) - v^s(\mathbf{y}))(u^0(\mathbf{x}) - u^0(\mathbf{y}))\gamma^t(\mathbf{x}, \mathbf{y}) \left.\frac{d}{dr}\right|_{r=t^+}$$

$$(\xi^r(\mathbf{x})\xi^r(\mathbf{y}))\, d\mathbf{y}d\mathbf{x}$$

$$+ \lim_{s,t\searrow 0} \frac{1}{2} \iint_{(\Omega\cup\Omega_I)^2} (v^s(\mathbf{x}) - v^s(\mathbf{y}))(u^0(\mathbf{x}) - u^0(\mathbf{y}))(\nabla_x\gamma^t(\mathbf{x}, \mathbf{y})^\top \mathbf{V}(\mathbf{x})$$

$$+ \nabla_y\gamma^t(\mathbf{x}, \mathbf{y})^\top \mathbf{V}(\mathbf{y}))\xi^t(\mathbf{x})\xi^t(\mathbf{y})\, d\mathbf{y}d\mathbf{x}$$

$$= \lim_{n\to\infty} \lim_{s,t\searrow 0} \frac{1}{2} \iint_{D_n} (v^s(\mathbf{x}) - v^s(\mathbf{y}))(u^0(\mathbf{x}) - u^0(\mathbf{y}))\gamma^t(\mathbf{x}, \mathbf{y}) \left.\frac{d}{dr}\right|_{r=t^+}$$

$$(\xi^r(\mathbf{x})\xi^r(\mathbf{y}))\, d\mathbf{y}d\mathbf{x}$$

$$+ \lim_{n\to\infty} \lim_{s,t\searrow 0} \frac{1}{2} \iint_{D_n} (v^s(\mathbf{x}) - v^s(\mathbf{y}))(u^0(\mathbf{x}) - u^0(\mathbf{y}))(\nabla_x\gamma^t(\mathbf{x}, \mathbf{y})^\top \mathbf{V}(\mathbf{x})$$

$$+ \nabla_y\gamma^t(\mathbf{x}, \mathbf{y})^\top \mathbf{V}(\mathbf{y}))\xi^t(\mathbf{x})\xi^t(\mathbf{y})\, d\mathbf{y}d\mathbf{x}$$

$$= \lim_{n\to\infty} \frac{1}{2} \iint_{D_n} (v^0(\mathbf{x}) - v^0(\mathbf{y}))(u^0(\mathbf{x}) - u^0(\mathbf{y}))\gamma(\mathbf{x}, \mathbf{y})(\text{div}\, \mathbf{V}(\mathbf{x}) + \text{div}\, \mathbf{V}(\mathbf{y}))\, d\mathbf{y}d\mathbf{x}$$

$$+ \lim_{n\to\infty} \frac{1}{2} \iint_{D_n} (v^0(\mathbf{x}) - v^0(\mathbf{y}))(u^0(\mathbf{x}) - u^0(\mathbf{y}))(\nabla_x\gamma(\mathbf{x}, \mathbf{y})^\top \mathbf{V}(\mathbf{x})$$

$$+ \nabla_y\gamma(\mathbf{x}, \mathbf{y})^\top \mathbf{V}(\mathbf{y}))\, d\mathbf{y}d\mathbf{x}$$

$$= \frac{1}{2} \iint_{(\Omega\cup\Omega_I)^2} (v^0(\mathbf{x}) - v^0(\mathbf{y}))(u^0(\mathbf{x}) - u^0(\mathbf{y}))\gamma(\mathbf{x}, \mathbf{y})(\text{div}\, \mathbf{V}(\mathbf{x}) + \text{div}\, \mathbf{V}(\mathbf{y}))\, d\mathbf{y}d\mathbf{x}$$

$$+ \frac{1}{2} \iint_{(\Omega\cup\Omega_I)^2} (v^0(\mathbf{x}) - v^0(\mathbf{y}))(u^0(\mathbf{x}) - u^0(\mathbf{y}))(\nabla_x\gamma(\mathbf{x}, \mathbf{y})^\top \mathbf{V}(\mathbf{x})$$

$$+ \nabla_y\gamma(\mathbf{x}, \mathbf{y})^\top \mathbf{V}(\mathbf{y}))\, d\mathbf{y}d\mathbf{x}$$

$$= \partial_t A(0, u^0, v^0)$$

Analogously to case 1, we obtain

$$\lim_{s,t \searrow 0} \partial_t G(t, u^0, v^s) = \lim_{s,t \searrow 0} \partial_t A(t, u^0, v^s) - \lim_{s,t \searrow 0} \partial_t F(t, v^s) + \lim_{t \searrow 0} \partial_t J(t, u^0)$$

$$= \partial_t A(0, u^0, v^0) - \partial_t F(0, v^0) + \partial_t J(0, u^0) = \partial_t G(0, u^0, v^0).$$

$\square$

Data availibility The code to get the results in Sect. 5 and the corresponding raw data from these experiments can be freely downloaded from https://github.com/schustermatthias/nlshape.

Declarations

Conflict of interest The authors declare that they have no conflict of interest.

References

1. Mardal, K.-A., Logg, A., Wells, G.N., et al.: Automated Solution of Differential Equations by the Finite Element Method. Springer, Berlin (2012)
2. Alnæs, M., Blechta, J., Hake, J., Johansson, A., Kehlet, B., Logg, A., Richardson, C., Ring, J., Rognes, M.E., Wells, G.N.: The FEniCS project version 1.5. Arch. Numer. Softw. **3**(100), 9–23 (2015)
3. Ameur, H.B., Burger, M., Hackl, B.: Level set methods for geometric inverse problems in linear elasticity. Inverse Prob. **20**(3), 673–696 (2004)
4. Andreu, F., Mazon, J.M., Rossi, J.D., Toledo, J.: Nonlocal Diffusion Problems. Mathematical Surveys and Monographs, vol. 165. AMS, Providence (2010)
5. Barlow, M.T., Bass, R.F., Chen, Z.-Q., Kassmann, M.: Non-local Dirichlet forms and symmetric jump processes. Trans. Am. Math. Soc. **361**(4), 1963–1999 (2009)
6. Bass, R.F., Kassmann, M., Kumagai, T.: Symmetric jump processes: localization, heat kernels and convergence. Ann. Inst. H. Poincaré Probab. Stat. **46**(1), 59–71 (2010)
7. Berggren, M.: A unified discrete-continuous sensitivity analysis method for shape optimization. In: Applied and Numerical Partial Differential Equations: Scientific Computing in Simulation, Optimization and Control in a Multidisciplinary Context, pp. 25–39. Springer (2009)
8. Fernández Bonder, J., Ritorto, A., Salort, A.: A class of shape optimization problems for some nonlocal operators. Adv. Calc. Var. **11**(4), 373–386 (2017)
9. Fernández Bonder, J., Spedaletti, J.F.: Some nonlocal optimal design problems. J. Math. Anal. Appl. **459**(2), 906–931 (2018)
10. Brockmann, D.: Anomalous diffusion and the structure of human transportation networks. Eur. Phys. J. Spec. Top. **157**(1), 173–189 (2008)
11. Brockmann, D., Theis, F.: Money circulation, trackable items, and the emergence of universal human mobility patterns. IEEE Pervasive Comput. **7**(4), 28–35 (2008)
12. Burchard, A., Choksi, R., Topaloglu, I.: Nonlocal shape optimization via interactions of attractive and repulsive potentials (2018). arXiv:1512.07282

13. Capodaglio, G., D'Elia, M., Bochev, P., Gunzburger, M.: An energy-based coupling approach to nonlocal interface problems. Comput. Fluids **207**, 104593 (2020)
14. Cusimano, N., Bueno-Orovio, A., Turner, I., Burrage, K.: On the order of the fractional Laplacian in determining the spatio-temporal evolution of a space-fractional model of cardiac electrophysiology. PLoS ONE **10**(12), 1–16 (2015)
15. Dalibard, A.-L., Gérard-Varet, D.: On shape optimization problems involving the fractional Laplacian. ESAIM Control Optim. Calc. Var. **19**(4), 976–1013 (2013)
16. Delfour, M.C., Zolésio, J.-P.: Shapes and Geometries: Metrics, Analysis, Differential Calculus, and Optimization. Advances in Design and Control. SIAM, Philadelphia (2011)
17. D'Elia, M., Glusa, C.: A fractional model for anomalous diffusion with increased variability. Analysis, algorithms and applications to interface problems. arXiv preprint arXiv:2101.11765 (2021)
18. D'Elia, M., Glusa, C., Otárola, E.: A priori error estimates for the optimal control of the integral fractional Laplacian (2018). arXiv:1810.04262
19. D'Elia, M., Gunzburger, M.: The fractional Laplacian operator on bounded domains as a special case of the nonlocal diffusion operator. Comput. Math. Appl. **66**(7), 1245–1260 (2013)
20. D'Elia, M., Gunzburger, M.: Optimal distributed control of nonlocal steady diffusion problems. SIAM J. Control. Optim. **52**(1), 243–273 (2014)
21. D'Elia, M., Gunzburger, M.: Identification of the diffusion parameter in nonlocal steady diffusion problems. Appl. Math. Optim. **73**(2), 227–249 (2016)
22. D'Elia, M., Gunzburger, M., Vollmann, C.: A cookbook for finite element methods for nonlocal problems, including quadrature rules and approximate Euclidean balls. arXiv preprint arXiv:2005.10775 (2020)
23. Du, Q.: Nonlocal Modeling, Analysis, and Computation. Society for Industrial and Applied Mathematics, Philadelphia (2019)
24. Du, Q., Gunzburger, M., Lehoucq, R.B., Zhou, K.: Analysis and approximation of nonlocal diffusion problems with volume constraints. SIAM Rev. **54**(4), 667–696 (2012)
25. Du, Q., Zhou, K.: Mathematical analysis for the peridynamic nonlocal continuum theory. ESAIM: M2AN **45**(2), 217–234 (2011)
26. D'Elia, M., Du, Q., Gunzburger, M., Lehoucq, R.B.: Nonlocal convection–diffusion problems on bounded domains and finite-range jump processes. Comput. Methods Appl. Math. **17**(4), 707–722 (2017)
27. D'Elia, M., Perego, M., Bochev, P., Littlewood, D.: A coupling strategy for nonlocal and local diffusion models with mixed volume constraints and boundary conditions. Comput. Math. Appl. **71**(11), 2218 – 2230 (2016). Proceedings of the conference on Advances in Scientific Computing and Applied Mathematics. A special issue in honor of Max Gunzburger's 70th birthday
28. Felsinger, M., Kassmann, M., Voigt, P.: The Dirichlet problem for nonlocal operators. Math. Z. **279**(3), 779–809 (2015)
29. Gal, C.G., Warma, M.: Nonlocal transmission problems with fractional diffusion and boundary conditions on non-smooth interfaces. Commun. Partial Differ. Equ. **42**(4), 579–625 (2017)
30. Geuzaine, C., Remacle, J.-F.: Gmsh: a 3-d finite element mesh generator with built-in pre- and post-processing facilities. Int. J. Numer. Methods Eng. **79**(11), 1309–1331 (2009)
31. Gilboa, G., Osher, S.: Nonlocal operators with applications to image processing. Multiscale Model. Simul. **7**(3), 1005–1028 (2009)
32. Glusa, C., D'Elia, M., Capodaglio, G., Gunzburger, M., Bochev, P.: An asymptotically compatible coupling formulation for nonlocal interface problems with jumps. arXiv preprint arXiv:2203.07565 (2022)
33. Guillemin, V., Pollack, A.: Differential Topology, vol. 370. American Mathematical Soc., Providence (2010)
34. Hintermüller, M., Ring, W.: A second order shape optimization approach for image segmentation. SIAM J. Appl. Math. **64**(2), 442–467 (2003)
35. Klar, M., Vollmann, C., Schulz, V.: A flexible 2d fem code for nonlocal convection-diffusion and mechanics (2022). arXiv:2207.03921
36. Laurain, A., Sturm, K.: Distributed shape derivative via averaged adjoint method and applications. ESAIM Math. Model. Numer. Anal. **50**(4), 1241–1267 (2016)
37. Levendorskiĭ, S.Z.: Pricing of the American put under lévy processes. Int. J. Theor. Appl. Finance **07**(03), 303–335 (2004)

38. Lou, Y., Zhang, X., Osher, S., Bertozzi, A.: Image recovery via nonlocal operators. J. Sci. Comput. **42**(2), 185–197 (2010)
39. Michor, P.W., Mumford, D.: Vanishing geodesic distance on spaces of submanifolds and diffeomorphisms. Doc. Math. **10**, 217–245 (2005)
40. Nocedale, J., Wright, S.J.: Numerical Optimization. Springer, New York (1999)
41. Parini, E., Salort, A.: Compactness and dichotomy in nonlocal shape optimization (2018). arXiv:1806.01165
42. Peyré, G., Bougleux, S., Cohen, L.: Non-local Regularization of Inverse Problems, pp. 57–68. Springer, Berlin (2008)
43. Rodriguez, G.E., Gimperlein, H., Stocek, J.: Nonlocal interface problems: modeling, regularity, finite element approximation, Preprint (2020). http://www.macs.hw.ac.uk/hg94/interface.pdf
44. Rosasco, L., Belkin, M., De Vito, E.: On learning with integral operators. J. Mach. Learn. Res. **11**, 905–934 (2010)
45. Schmidt, S.: Efficient large scale aerodynamic design based on shape calculus. Ph.D. thesis, Universiät Trier (2010)
46. Schmidt, S., Ilic, C., Schulz, V., Gauger, N.: Three dimensional large scale aerodynamic shape optimization based on the shape calculus. AIAA J. **51**(11), 2615–2627 (2013)
47. Schulz, V., Siebenborn, M.: Computational comparison of surface metrics for PDE constrained shape optimization. Comput. Methods Appl. Math. **16**(3), 485–496 (2016)
48. Schulz, V., Siebenborn, M., Welker, K.: Structured inverse modeling in parabolic diffusion problems. SIAM J. Control. Optim. **53**(6), 3319–3338 (2015)
49. Schulz, V., Siebenborn, M., Welker, K.: Efficient PDE constrained shape optimization based on Steklov–Poincaré-type metrics. SIAM J. Optim. **26**(4), 2800–2819 (2016)
50. Schulz, V., Siebenborn, M., Welker, K.: A novel Steklov–Poincaré type metric for efficient PDE constrained optimization in shape spaces. SIAM J. Optim. **26**(4), 2800–2819 (2016)
51. Seleson, P., Gunzburger, M., Parks, M.L.: Interface problems in nonlocal diffusion and sharp transitions between local and nonlocal domains. Comput. Methods Appl. Mech. Eng. **266**, 185–204 (2013)
52. Siebenborn, M.: A shape optimization algorithm for interface identification allowing topological changes. J. Optim. Theory Appl. **177**(2), 306–328 (2018)
53. Siebenborn, M., Vogel, A.: A shape optimization algorithm for cellular composites (2019). arXiv:1904.03860
54. Silling, S.A.: Reformulation of elasticity theory for discontinuities and long-range forces. J. Mech. Phys. Solids **48**(1), 175–209 (2000)
55. Sire, Y., Vázquez, J.L., Volzone, B.: Symmetrization for fractional elliptic and parabolic equations and an isoperimetric application. Chin. Ann. Math. Ser. B **38**(2), 661–686 (2017)
56. Sokolowski, J., Zolésio, J.-P.: Introduction to Shape Optimization. Springer, Berlin (1992)
57. Sturm, K.: Minimax Lagrangian approach to the differentiability of nonlinear pde constrained shape functions without saddle point assumption. SIAM J. Control Optim. **53**(4), 2017–2039 (2015)
58. Sturm, K.: On shape optimization with non-linear partial differential equations. Ph.D. thesis, Technische Universiät Berlin (2015)
59. Tankov, P.: Financial Modelling with Jump Processes. CRC Press, Cambridge (2003)
60. Tian, X.: Nonlocal models with a finite range of nonlocal interactions. Ph.D. thesis, Columbia University (2017). https://doi.org/10.7916/D8ZG6XWN
61. Vollmann, C.: Nonlocal models with truncated interaction kernels—analysis, finite element methods and shape optimization. Ph.D. thesis, Universität Trier (2019). https://ubt.opus.hbz-nrw.de/frontdoor/index/index/docId/1225
62. Welker, K.: Efficient PDE constrained shape optimization in shape spaces. Ph.D. thesis, Universität Trier (2016). http://ubt.opus.hbz-nrw.de/volltexte/2017/1024/
63. Welker, K.: Suitable spaces for shape optimization (2017). arXiv:1702.07579
64. Zhou, K., Du, Q.: Mathematical and numerical analysis of linear peridynamic models with nonlocal boundary conditions. SIAM J. Numer. Anal. **48**(5), 1759–1780 (2010)